Hemispheric divergence of interoceptive processing across psychiatric disorders

Emily M. Adamic[1,2], Adam R. Teed[1], Jason A. Avery[3], Feliberto de la Cruz[4], Sahib S. Khalsa[1,5]

[1]Laureate Institute for Brain Research, Tulsa, OK, USA, 74136
[2]Department of Biological Sciences, University of Tulsa, Tulsa, OK, USA, 74104
[3]Laboratory of Brain and Cognition, National Institute of Mental Health, Bethesda, MD, USA, 20814
[4]Laboratory for Autonomic Neuroscience, Imaging, and Cognition (LANIC), Department of Psychosomatic Medicine and Psychotherapy, Jena University Hospital, Jena, Thuringia, Germany, 07743
[5]Oxley College of Health Sciences, University of Tulsa, Tulsa, OK, USA, 74119

Correspondence:
Sahib Khalsa MD, PhD
skhalsa@laureateinstitute.org

Abbreviated title: Hemispheric divergence of interoception

Version date: May 6, 2024

Abstract

Interactions between top-down attention and bottom-up visceral inputs are assumed to produce conscious perceptions of interoceptive states, and while each process has been independently associated with aberrant interoceptive symptomatology in psychiatric disorders, the neural substrates of this interface are unknown. We conducted a preregistered functional neuroimaging study of 46 individuals with anxiety, depression, and/or eating disorders (ADE) and 46 propensity-matched healthy comparisons (HC), comparing their neural activity across two interoceptive tasks differentially recruiting top-down or bottom-up processing within the same scan session. During an interoceptive attention task, top-down attention was voluntarily directed towards cardiorespiratory or visual signals, whereas during an interoceptive perturbation task, intravenous infusions of isoproterenol (a peripherally-acting beta-adrenergic receptor agonist) were administered in a double-blinded and placebo-controlled fashion to drive bottom-up cardiorespiratory sensations. Across both tasks, neural activation converged upon the insular cortex, localizing within the granular and ventral dysgranular subregions bilaterally. However, contrasting hemispheric differences emerged, with the ADE group exhibiting (relative to HCs) an asymmetric pattern of overlap in the left insula, with increased or decreased proportions of co-activated voxels within the left or right dysgranular insula, respectively. The ADE group also showed less agranular anterior insula activation during periods of bodily uncertainty (i.e., when anticipating possible isoproterenol-induced changes that never arrived). Finally, post-task changes in insula functional connectivity were associated with anxiety and depression severity. These findings confirm the dysgranular mid-insula as a key cortical interface where attention and prediction meet real-time bodily inputs, especially during heightened awareness of interoceptive states. Further, the dysgranular mid-insula may indeed be a “locus of disruption” for psychiatric disorders.

Introduction

Maintaining the body in a physiologically optimal state is a primary function of the mammalian nervous system. The neurovisceral architecture accomplishing such feats depends on the hierarchical central processing of peripheral internal body signals and operates hierarchically and across heterogenous time scales (Smith et al. 2017), automatically returning the internal state to a setpoint (i.e., homeostasis) (Cannon 1939) or shifting the internal state away from a setpoint in anticipation of future deviations (i.e. allostasis) (Sterling 2012). Importantly, these regulatory operations may depend on the unconscious as well as conscious monitoring of interoceptive states. Interoceptive sensations may even dominate awareness during significant physiological disturbances, motivating behaviors that restore bodily states to homeostatic equilibrium (Khalsa and Lapidus 2016) and forming the basis for emotional experience and numerous cognitive processes (Adolfi et al. 2017; Carvalho and Damasio 2021; Critchley and Garfinkel 2017; Uddin et al. 2014). In turn, dysfunctional interoception has been implicated in the pathophysiology of psychiatric (Bonaz et al. 2021; Khalsa et al. 2018) and neurological disorders (Birba et al. 2022; Drane et al. 2020), underscoring the importance of identifying the form and function of interoceptive neurocircuitry in humans, particularly in relation to conscious experience of the inner body.

Conscious interoceptive perceptions must, to a considerable extent, reflect the organism's current physiological state. This is hierarchically conveyed to the brain by cascades of peripheral interoceptive inputs, from vagal and spinal afferent nerves relaying signals transduced from interoceptors located throughout the major internal organ systems (e.g., cardiovascular, respiratory, gastrointestinal, urogenital), as well as via direct chemohumoral signaling (Berntson and Khalsa 2021). Ascending interoceptive pathways converge via brainstem and thalamic nuclei onto the insular cortex, a structurally and functionally diverse region suggested to be the integrative hub for interoceptive awareness, emotional feelings, and overall body awareness (Craig 2002, 2009) (for discussions of additional pathways and cortical targets see (Berntson and Khalsa 2021; Khalsa et al. 2009; Mayeli et al. 2023). A principal role for the insular cortex in interoceptive awareness is supported by previous functional neuroimaging studies from our group, which have highlighted the insula as the primary region dynamically tracking pharmacological perturbations of the heart and lungs in both healthy individuals (Hassanpour et al. 2016, 2018), and those with generalized anxiety disorder (Teed et al. 2022) (for fMRI meta-analyses of cardiac and gastrointestinal interoception findings see Schulz (2016) and Halani et al. (2020), respectively). Our studies have identified multiple subregions of the insula in this "bottom-up" processing of afferently relayed cardiorespiratory signals, including the dysgranular mid and granular posterior sectors, in general agreement with existing theoretical (Barrett and Simmons 2015; Fermin, Friston, and Yamawaki 2022) and cytoarchitectonic (Evrard 2019) arguments regarding their function.

While cortical sensitivity to ascending signals is presumptively required for conscious detection of internal physiological shifts in humans, accumulating evidence also suggests that subjective perceptions (in any sensory modality) are not simply veridical reflections of these ascending inputs, faithfully transmitted and reproduced in a dormant sensory cortex (Clark 2013; Corbetta, Patel, and Shulman 2008; Mechelli et al. 2004; Pace-Schott et al. 2019). Instead, intrinsic "top-down" processes also appear to modulate the activity of sensory cortices (including the insula), potentially altering the resulting percept in the process. For example, internal models of the

body that anticipate the sensory consequences of descending regulation can adjust the precision-weighting of prediction error signals in a context-specific manner, increasing or decreasing the sensory processing of interoceptive inputs (Clark 2016; Petzschner et al. 2021; Pezzulo, Barca, and Friston 2015; Seth and Friston 2016). Extending beyond these model-based influences are goal-directed activities (also described previously as the 'attentional spotlight' effect (Brefczynski and DeYoe 1999)), whereby focusing voluntary attention towards certain environmental signals not only alters their conscious experience but selectively enhances neural activity in the responsive area of cortex. With respect to interoception, such goal-directed shifts in attention towards endogenous visceral signals have consistently identified activation of the mid insular cortex in healthy individuals (Avery et al. 2017; Simmons et al. 2013), and revealed abnormal mid insula activity associated with symptoms in those with eating disorders (Kerr et al. 2016), depression (Avery et al. 2014; Burrows et al. 2022), and substance use disorders (Stewart et al. 2020).

Conscious perceptions of interoceptive signals are thus underpinned by reciprocal interactions between bottom-up, ascending interoceptive afferents and the coupled, top-down descending efferent systems that enact adaptive regulation and attentional control (Berntson and Khalsa 2021). Based on the available evidence, the insula is uniquely positioned to serve as a cortical interface between these two information streams for the processing of interoceptive signals. The highly interconnected nature of the mammalian insula with other cortical (prefrontal (Mufson and Mesulam 1982), somatosensory (Augustine 1996), cingulate (Mufson and Mesulam 1982) cortices), subcortical (amygdala, thalamus (Gehrlach et al. 2020)), and brainstem (Gogolla 2017) areas facilitates the ability for salient bottom-up activity to recruit conscious attention mechanisms and/or give rise to perceptions and feelings that can adaptively drive behavior and promote homeostatic regulation (Evrard 2019). Furthermore, disrupted processing in this region may be characteristic of individuals with certain psychiatric disorders. In a previous human functional magnetic resonance imaging (fMRI) meta-analysis, abnormal activation of the left dorsal mid-insula differentiated healthy individuals from groups of individuals with anorexia nervosa, anxiety disorders, depression, bipolar disorder, or schizophrenia, across tasks involving the bottom-up modulation of pain, dyspnea, or hunger or the top-down manipulation of interoceptive attention (Nord, Lawson, and Dalgleish 2021). This insular "locus of disruption" was inferred as a possible transdiagnostic and domain-general neuromarker of psychopathology, and the finding advanced the field by pointing toward the mid-insula as an important area for interoceptive dysfunction and a putative target for clinical intervention (Paulus and Khalsa 2021). Despite the theoretical and empirical convergence related to bottom-up and top-down processing in the insula , no study to date has directly investigated both interoceptive processing streams together in the same sample.

Here, we conducted a pre-registered conjunction analysis of two established neuroimaging tasks preferentially manipulating the assessment of top-down and bottom-up interoception (Adamic et al. 2021). Our hypotheses, based on a voxelwise whole-brain approach, were threefold: 1) broad regions of the dysgranular mid insula would be co-activated when a) engaging top-down interoceptive attention under physiological resting conditions and b) during bottom-up perturbation of peripheral interoceptive signals via the adrenergic drug isoproterenol, 2) the agranular anterior insula would be preferentially selective to manipulations of interoceptive uncertainty, such as those occurring during saline infusions, and 3) relative to healthy individuals,

156 interoceptive processing in the insula would show lateralized differences across a transdiagnostic
157 group of individuals with anxiety, depression, and/or eating disorders. To extend the functional
158 interpretation of convergence, the convergent dysgranular insula regions identified in the initial
159 analysis were used as seeds in an exploratory whole-brain resting state functional connectivity (FC)
160 analysis. Finally, divergent voxels selective to the engagement of top-down expectancies about the
161 body were isolated, focusing on temporal windows of the ISO task when the anticipation of
162 potential interoceptive change was maximal. We predicted that the agranular insula would be
163 preferentially engaged during these windows, and not engaged during the peak of perturbation or
164 during interoceptive attention alone.
165

166 **Methods**

167 ***Participants***

168 Seventy individuals with primary diagnoses of anxiety, depression, and/or eating disorders
169 (ADE) and 57 healthy comparisons (HC) were included in the study. Diagnoses were based on DSM-
170 5 criteria using the Mini-International Neuropsychiatric Interview (Sheehan et al. 1998). Comorbid
171 anxiety and depression were allowed, but those with panic disorder were excluded to reduce the
172 likelihood of isoproterenol-induced panic anxiety (Pohl et al. 1988) in the scanner. Participants
173 with a primary diagnosis of anxiety were further required to have scores greater than seven for the
174 GAD-7 (Spitzer et al. 2006) and greater than 10 for the Overall Anxiety Severity and Impairment
175 Scale (OASIS) (Campbell-Sills et al. 2009), indicative of clinically significant anxiety levels.
176 Participants with eating disorders were required to have met lifetime DSM-5 criteria for anorexia
177 nervosa but were required to be weight restored as defined by a minimum body mass index of 18.5
178 or greater for at least 1 month to control for the well-described state effects of acute starvation on
179 neural activation (Wierenga et al. 2015). We used several self-report scales to measure symptom
180 severity across the sample due to our interest in transdiagnostic markers of pathology.
181 Psychotropic medications were allowed as long as there was no change in dosage during the four
182 weeks preceding the MRI. Finally, a medical evaluation including a 12-lead electrocardiogram read
183 by a cardiologist ensured all participants were generally healthy, free of cardiorespiratory,
184 endocrine, metabolic, or other illnesses, as well as free of major neurological disorders or other
185 psychiatric disorders besides ADE. Additional exclusion criteria involved anything that would
186 render the participant unfit for the MRI environment, such as inability to remove body piercings or
187 implanted electrodes. The study was part of a larger project investigating interoception in anorexia
188 nervosa and generalized anxiety disorder (ClinicalTrials.gov Identifier: NCT02615119). Additional
189 recruitment, screening, and exclusion information can be found in (Teed et al. 2022), which used a
190 subset of the current sample for a separate analysis.
191 All study procedures were approved by the Western Institutional Review Board, and all
192 participants provided written informed consent before participation. All data were collected at the
193 Laureate Institute for Brain Research in Tulsa, OK.
194

195 ***Experimental design and statistical analysis***

During a single scanning session, participants completed two fMRI tasks designed to preferentially assess intersecting aspects of cardiorespiratory interoception while measuring blood oxygen level-dependent (BOLD) signals (Figure 1). The Isoproterenol Infusion (ISO) task was always performed before the Visceral Interoceptive Attention (VIA) task, which we considered to preferentially emphasize the bottom-up or top-down processing of interoceptive signals, respectively. The fixed order of these tasks reflected the project's primary emphasis on acquiring the infusion data. Complete details of these paradigms are described in the following sections. Both tasks were immediately preceded by and followed by an eight-minute eyes-open resting state scan. For the resting state scans, participants were instructed to remain as still as possible, to keep their eyes open and fixated on a white cross centered upon a dark screen, and to "clear your mind and do not think about anything in particular." To minimize head motion during scanning, a layer of tape was gently placed over the participant's forehead to provide them with tactile feedback regarding head position. Cardiac and respiratory activity was measured simultaneously at 40Hz during all scans using a pulse oximeter and thoracic respiratory belt, respectively. Finally, participants completed a high-resolution anatomical MRI scan before any resting state or task-based imaging data was collected.

Isoproterenol Infusion Task

Intravenous bolus infusions of the peripherally-acting beta-adrenergic agonist isoproterenol (ISO) were used to manipulate afferent interoceptive signals in a bottom-up fashion. Infusions of 2.0 micrograms (mcg), 0.5 mcg, or Saline were administered 60 seconds into each four-minute infusion scan as per Hassanpour et al. (Hassanpour et al. 2018) and Teed et al. (Teed et al. 2022). Infusion delivery was randomized, double-blinded, and repeated twice for each dose for a total of six infusions (*i.e.,* six infusion scans). Throughout each infusion scan, participants were instructed to focus their attention on the sensations from their heart and lungs while providing real-time, continuous intensity ratings using an MRI-compatible dial (Current Designs Inc.) with their dominant hand, the rating of which was visible to them on the screen while scanning. The intensity rating scale ranged from 0 (none or normal) to 10 (most ever). Thus, this task engaged top-down attention towards cardiorespiratory sensations while parametrically perturbing the bottom-up stream in the ISO trials, with an absence of such perturbation in Saline trials. Following our lab's previous studies (Hassanpour et al. 2018; Teed et al. 2022) we split the time course of this task into pre-defined epochs of interest, and focused on the Anticipation period (seconds 60 to 80, directly following the infusion but before the ISO-induced rise in heart rate) and the Peak period (seconds 80 to 120, encompassing the onset and peak magnitude of ISO-induced heart rate change), and contrasted these with the Baseline period (the initial 45 seconds of the task). Following each scan, participants also retrospectively reported the intensity of perceived cardiac or respiratory sensations, separately, that they felt during the scan, as well as their anxiety or excitement. To familiarize participants with the task and isoproterenol-induced sensations, single-blinded infusions of 1mcg ISO and Saline (one trial each) were given before the MRI session.

Visceral Interoception Attention Task

The Visceral Interoceptive Attention (VIA) task was used to assess the top-down attentional processing of interoceptive signals at rest (*i.e.,* no infusions were delivered). This minimalistic task, adapted from Simmons et al. (Simmons et al. 2013), involved repeated trials of interoceptive or exteroceptive attention delivered across three six-minute runs, with the order of these runs randomized across participants. During the interoceptive attention trials, the words "HEART", "LUNGS", or "STOMACH" were presented on the screen for eight seconds, during which participants were instructed to focus their attention on the naturally-occurring sensations experienced from that organ. During the exteroceptive attention control trials, the word "TARGET" was shown on the screen at changing shades of black to grey, and participants were instructed to pay attention to the degree of color change. After half of all trials in each condition participants were asked to indicate via an MRI-compatible button box the intensity of sensations they had perceived from that organ (interoceptive condition) or the intensity of the color change (exteroceptive condition) on a rating scale of 1 (no sensation/no change in color) to 7 (high intensity).

MRI data acquisition

All scans were conducted in a 3 Tesla General Electric scanner with an eight-channel head coil (GE MR750; GE Healthcare). Anatomical images were acquired via T1-weighted, magnetization-prepared, rapid gradient-echo sequences images (MPRAGE). MPRAGE parameters were: 190 axial slices, slice thickness = 0.9mm, TR/TE = 5/2.012 ms, FOV = 240 x 192mm^2, matrix size 256 x 256, flip angle 8 degrees, inversion time 725 ms, SENSE acceleration R =2, with a sampling bandwidth of 31.2. For the task-based and resting state functional scans, T2*-weighted images were acquired via an echoplanar sequence of the following parameters: single-shot gradient echo planar imaging (EPI) sequence covering the whole brain, obtaining 39 axial slices, 2.9mm thick with no gap and a voxel size of 1.875 x 1.875 x 2.9mm^3, with TR/TE = 2000/27ms, FOV = 240 x 240mm^2, flip angle 78 degrees, SENSE acceleration R = 2 with a 96 x 96 matrix.

fMRI task-based analysis

Each task was analyzed separately in AFNI (Cox 1996), following the previously-published preprocessing pipelines specific to each task (Simmons et al. 2013; Teed et al. 2022). Preprocessing steps common to both tasks included removal of the first four volumes (ISO) or five volumes (VIA) for steady state tissue magnetization, despiking, slice time correction, spatial smoothing (6mm full width at half maximum Gaussian kernel), co-registration to the first volume, scaling of each voxel, and normalization to Talairach space. In the ISO task, temporal fluctuations of cardiac and respiratory frequencies and their first-order harmonics were additionally removed from the imaging data using RETROICOR, implemented via custom code in MATLAB (MathWorks).

After preprocessing, whole-brain individual-level activation maps were created. For the ISO task, this involved regressing out baseline drift and contrasting average BOLD percent signal change (PSC) within each epoch of interest (Anticipation and Peak, separately) against the average PSC during the Baseline period. For the VIA task, this involved a multiple linear regression model that included terms for baseline drift, six motion parameters, and each interoceptive and exteroceptive attention condition, and contrasting PSC associated with cardiorespiratory attention (*i.e.,* collapsed across "Heart" and "Lung" trials) against that of exteroceptive attention ("Target"

control condition). This cardiorespiratory contrast was specifically chosen as it best matched the cardiorespiratory perturbation induced by ISO.

After the creation of individual-level maps, quality control checks were performed. Participants were excluded from further group analysis if they had poor quality imaging data according to the previously established approaches in each task. For the ISO task, individual runs were excluded if more than 20% of all time points had over 0.3mm motion, based on the Euclidean norm of the six motion parameters; following this, participants were excluded who were missing both runs of the Saline or 2.0mcg doses. For the VIA task, all time points with an outlier fraction greater than 5% or an estimated motion greater than 0.3mm were censored, and any run in which this censoring removed over 20% of volumes was excluded. If a participant was missing two or more VIA runs (out of three), they were removed from the analysis. To avoid an unbalanced conjunction analysis in the following step, participants excluded from one task were also removed from the other task. The groups were then propensity matched based on age, sex, and BMI to equalize the sample sizes (*MatchIt* function in R), resulting in a final sample of participants who had high quality imaging data in *both* tasks.

Using this propensity-matched sample, group-level statistical activation maps were created for each task and group separately, using whole-brain voxel-wise t-tests (*3dttest++* in AFNI) with Equitable Threshold And Clustering corrections for an overall False Positive Rate of 5% (Cox 2019). With these group activation maps, we were thus able to identify voxels significantly active at the group level in each experimental condition.

Convergence maps

To examine voxels co-activated across the ISO and VIA tasks, we restricted the functional neuroimaging analysis to the specific portions of each task that best exemplified the interoceptive processes of interest: namely, Heart + Lung interoceptive attention relative to exteroceptive attention in the VIA task, and the Peak period of the 2.0mcg dose relative to the Baseline period in the ISO task. We narrowed the focus of analysis to this specific time period and dose of the ISO task because it represents, as shown in previous studies, the peak level of cardiorespiratory perturbation that can be confidently ascertained by subjective report in all individuals (Hassanpour et al. 2018; Teed et al. 2022). Using the statistically-thresholded group activation maps from each task, binarized into active and non-active voxels, we created convergence maps by joining the binary maps across the specified contrasts of each task. These convergence maps thus identified which voxels were commonly activated, *i.e.*, *convergent*, at the group level during both tasks. Due to our pre-specified focus on cytoarchitectural processing of the insular cortex, we subdivided these convergence maps (after converting to MNI space) into three bilateral insular subregions of interest, defined using the Brainnetome probabilistic cytoarchitectonic atlas (Fan et al. 2016), as follows: agranular anterior (regions 165 and 167 for the left hemisphere, 166 and 168 for the right), dysgranular mid (regions 169 and 173 for the left hemisphere, 170 and 174 for the right), and granular posterior (region 163 and 171 for the left hemisphere, 164 and 172 for the right).

Each convergence map was evaluated in four ways: 1) the spatial extent of convergence (*i.e.,* number of convergent voxels) within each insular subregion, tested for group differences via chi-square tests, 2) the spatial similarity of patterns of convergence between HC versus ADE groups,

measured via Dice coefficient separately for each hemisphere (using AFNI's *3ddot*), 3) the degree of task overlap within each group and hemisphere separately, quantified via the overlap coefficient (*i.e.,* the proportion of the ISO cluster overlapping with the VIA cluster, as per (Bowring, Maumet, and Nichols 2019), and finally 4) the average PSC across convergent voxels within each cytoarchitectonic subregion, compared across groups and hemispheres using linear mixed effects regression (*lmerTest* library in R, with the following equation: percent signal change ~ group * hemisphere + (1|subject)). In this linear model, the fixed effects of group and hemisphere were tested with respect to the magnitude of activation within subregion-specific convergent voxels, and significant main effects were interpreted using post-hoc contrasts between the estimated marginal means of each condition (*emmeans* library in R). Additionally, linear regression was used to examine possible associations between PSC in hemisphere- and subregion-specific convergent voxels and the following variables: trait measures of anxiety and depression, the objective degree of peripheral perturbation (*i.e.,* mean change in heart-rate during the Peak period of the 2.0mcg dose), real-time subjective rating of cardiorespiratory intensity (*i.e.,* mean change in dial rating during the Peak period of the 2.0mcg dose), and retrospective ratings of cardiac and respiratory intensity, anxiety, and excitement following the 2.0mcg dose. For these associations, we used a dimensional approach that collapsed across groups, considering all participants on a continuous scale.

fMRI resting state analysis

In an exploratory whole-brain resting state functional connectivity (FC) analysis, we aimed to identify which connections, if any, between convergent regions and the rest of the brain were altered following the interoceptive manipulations, and if these patterns of connectivity change differed between groups. We predicted that residual group-specific changes in functional connectivity of the insular regions activated during the ISO and VIA tasks would be present in the resting state scan at the end of the scanning session, reflecting additional neural signatures of interoceptive processing. We did not include a temporal control condition for this exploratory analysis, and thus we were unable to examine the specificity of insular connectivity changes across time in relation to test-retest reliability measures of the group's resting state data.

Resting state scans were analyzed in AFNI with a preprocessing pipeline optimized for connectivity analysis. After discarding the first five images to ensure steady-state tissue magnetization, we removed spikes in the signal intensity time course, and removed physiological noise using respiration volume per time (RVT) (Birn et al. 2008) and RETROICOR (Glover, Li, and Ress 2000) regressors that model slow blood oxygenation level fluctuations and time-locked cardiac and respiratory artifacts, respectively. The RVT regressors consisted of the RVT function and four delayed terms at 5, 10, 15, and 20 seconds, and the RETROICOR regressors consisted of four respiratory and four cardiac generated on a slice-wise basis by AFNI's "RetroTS.m" script (Jo et al. 2010). Further preprocessing steps included slice-timing correction, rigid body realignment, warping to MNI space, and smoothing with a 6-mm full-width half-maximum Gaussian kernel. Next, we applied a high-pass filter to remove all non-relevant ultra-slow fluctuations below 0.01 Hz, and then further reduced potential contributions of non-neural sources by regressing out the following nuisance variables: (1) 12 head motion regressors (6 realignment parameters and their derivatives), (2) voxel-wise local white matter regressors, and (3) three principal components of ventricle signals (ANATICOR). Following preprocessing, any subject with greater than 10% of

volumes above our motion cut-off of 0.3mm for the Euclidean norm of the motion derivatives was excluded from further analysis.

From the pre- and post-interoception resting state scans, time series were extracted from the convergent ROIs within the left and right hemispheres for HC and ADE groups separately, and correlated these respective time series against those of all other voxels in the brain to create an FC map for each resting state period (i.e., pre- and post-interoception). The resulting correlation coefficients were converted to Fisher z-statistics to produce a more normally distributed variable. To examine group differences in the effect of time (*i.e.,* pre- versus post-interoception tasks) on resting state FC, all resulting clusters of this group*time interaction analysis were corrected for multiple comparisons using the *3dClustSim* function in AFNI, using 10,000 Monte Carlo simulations of whole-brain fMRI data to determine the cluster size at which the false positive probability was below $\alpha<0.05$ with an uncorrected voxel-wise threshold of $p<0.001$, yielding a threshold of 150 contiguous voxels. This approach allowed the identification of regions that changed connectivity with the convergent insula differently for HC vs. ADE groups following top-down and bottom-up interoception. Finally, we conducted a correlational analysis to examine whether individual changes in FC were related to trait measures of anxiety and depression in the transdiagnostic sample, using the Bonferroni method for multiple comparison correction. These correlations were performed to help interpret the functional significance of residual changes, based on previous studies showing trait-related differences following interoception (De la Cruz et al. 2023).

Divergence maps

To isolate voxels selective to the engagement of top-down expectancies about the body, we focused on specific time windows of the ISO task were where expectations of potential interoceptive change were preferentially engaged: namely, the Anticipation period across all doses, and the Peak period of the Saline dose. The Anticipation period covered the 20 second epoch right after the intravenous infusion was delivered but before the onset of any cardiorespiratory perturbation (in the case of an isoproterenol dose administration). Thus, the Anticipation period represented a time when no peripheral change was occurring, but also one where participants were unsure about whether or not such a change was coming. This state of uncertainty would continue into the Peak period of the Saline dose, where again, no peripheral physiological change was induced. In the setting of isoproterenol dose administration, this state of uncertainty would resolve when participants correctly identified and rated the onset of changes in cardiorespiratory sensation. Based on previous studies from our lab using this task, we expected that by the end of the Saline Peak window some participants would update their beliefs about what had occurred after realizing that they had not reported experiencing a cardiorespiratory perturbation (i.e., their dial ratings remained at zero). Together, the Anticipation period and the ensuing Peak period of the Saline dose share some similarities with the VIA task in their involvement of top-down interoceptive attention during physiological rest, but critically, they differ in their added expectancies about possible changes in the state of the body. Thus, by isolating voxels preferentially active during these ISO anticipatory windows that were not active during VIA top-down attention alone, it we presumed it would be possible to separate the effect of bodily expectancies from the general effect of bodily attention.

For this aim, group-level activation maps from the Anticipation period (averaged across all doses) and the Peak period of the Saline dose, both relative to the Baseline period, were examined. Like the convergence map approach described above, these maps were binarized within each period and group separately, transformed to MNI space, reduced to the cytoarchitecturally-subdivided insular cortex, and joined with the binarized activation map for the Heart and Lung relative to Target contrast in the VIA task. Here, our focus was instead on the *divergent* voxels, *i.e.,* on those that were active only during specific periods of the ISO task and that were not co-active during the VIA task. As per our hypothesis regarding anterior insula involvement in interoceptive expectancy processing, these "ISO task only" voxels were restricted to those within the agranular anterior insula, and were evaluated in two ways: 1) spatial extent of activation (*i.e.,* number of voxels) across groups, time periods, and hemispheres, examining differences via chi-square tests with Bonferroni correction for multiple comparisons, and 2) magnitude of activation, examining differences in average PSC across the fixed effects of group, hemisphere, and time period using linear mixed effects regression and interpreting significant main effects using post-hoc contrasts of estimated marginal means (as previously described). Finally, we examined possible associations between average PSC in these expectancy-specific agranular regions and trait measures of anxiety using linear regression, transdiagnostically across groups.

Physiological and behavioral analysis

To test for group differences in the time courses of heart rate and real-time dial ratings during the ISO task (2.0mcg isoproterenol and Saline infusions), we used cluster-based permutation testing (*permutes* package in R) separately for each dose after averaging across both trials. A significant group difference was defined as any contiguous set of time points (two or more continuous seconds) where permutation testing revealed a statistical difference at $p<0.05$. We used linear regression transdiagnostically to test if the magnitude of heart rate or dial rating change, when averaged across each epoch of interest, was associated with dimensional measures of trait anxiety and depression across groups. Finally, we used two-tailed t-tests separately for each task and condition to test group differences in retrospective ratings of interoceptive intensity, anxiety, and excitement in the ISO task and interoceptive and exteroceptive intensity in the VIA task. This approach reflected our primary interest in investigating group differences in perceptual ratings, rather than performing additional within-group comparisons across modalities or doses.

Code accessibility

Custom AFNI and R scripts are posted on the Open Science Framework preregistration for this project (Adamic et al. 2021).

Results

Of the 127 total participants included in this study, 57 ADE individuals and 46 HC individuals fulfilled criteria for high-quality brain imaging data with both tasks. In line with the predominant female prevalence of these disorders, most of the participants were female. To obtain

447 equal-sized groups for group-level comparison, propensity matching on age, self-reported sex, and
448 body mass index resulted in 46 individuals per group (Table 1). After propensity matching, the two
449 groups were not significantly different regarding age, body mass index, and sex, but they differed
450 significantly on trait measures of anxiety (State-Trait Anxiety Inventory; STAI), anxiety sensitivity
451 (Anxiety Sensitivity Index; ASI, Total and subscales), depression (Patient Health Questionnaire-9;
452 PHQ-9) (Kroenke, Spitzer, and Williams 2001), and eating disorders (Sick, Control, One, Fat, Food
453 questionnaire; SCOFF) (Kutz et al. 2020). All participants in the ADE group exhibited some form of
454 psychiatric comorbidity. Across the group, 67% had a diagnosis of GAD (current or lifetime), 72%
455 of major depression (current or remitted), and 35% of anorexia nervosa (current or lifetime). Most
456 ADE participants reported taking psychiatric medication (see Table 1 for details).
457
458 ***Convergence analysis***

459 Bilateral patches of the ventral mid-insular cortex were commonly activated during the ISO
460 and VIA tasks (Figure 2) (Table 2). Quantification of the spatial extent of this convergence in the
461 pre-defined probabilistic agranular, dysgranular and granular subregions revealed that these
462 convergent clusters were localized primarily to the dysgranular insula bilaterally (Figure 3A), but
463 with a hemispheric asymmetry across groups: the ADE group showed a greater proportion of
464 overlapping voxels within the left dysgranular insula (χ^2_1 = 26.7, p<0.001 for group comparison)
465 whereas the HC group showed a greater number of overlapping voxels within the right dysgranular
466 insula (χ^2_1 = 26.7, p<0.001 for group comparison) (Figure 3B). Correspondingly, the spatial
467 similarity of these convergently activated voxels between the groups was lower for the left
468 dysgranular insula (Dice coefficient of 0.58) than for the right (Dice coefficient of 0.78) (Figure 2).
469 In addition to these group hemispheric differences in spatial extent, there was a lower amount of
470 overlap between the two tasks in the left dysgranular insula for both groups (left hemisphere
471 overlap coefficients: 0.42 and 0.63 for HC and ADE, respectively; right hemisphere overlap
472 coefficients: 0.83 and 0.78, for HC and ADE, respectively).
473 Despite these group differences in the spatial extent and spatial similarity of convergence,
474 the magnitude of activation within convergent dysgranular subregions during the Peak of
475 perturbation (ISO 2.0mcg dose) or Heart and Lung attention (VIA task) was not different between
476 groups ($F_{1,90}$ = 0.64 and 0.05, p = 0.43 and 0.82 for main effect of group in ISO and VIA tasks,
477 respectively). However, during both of these task conditions, activation was greater within the right
478 hemisphere than the left ($F_{1,90}$ = 6.13 and 5.10, p = 0.015 and 0.027 for main effect of hemisphere
479 during ISO and VIA tasks, respectively; t_{90} = -2.48 and -2.25, p = 0.02 and 0.03 for post-hoc contrasts
480 between the left versus right hemisphere when collapsed across groups) (Figure 4A). This
481 hemispheric effect on activation magnitude was specific to interoceptive processing, as no similar
482 hemispheric difference was seen during the exteroceptive condition of the VIA task ($F_{1,90}$ =0.68,
483 p=0.41). Furthermore, the magnitude of activation within the right (but not the left) dysgranular
484 convergent region during the peak of cardiorespiratory perturbation was associated with the
485 intensity of real-time cardiorespiratory sensations (*i.e.,* mean dial rating) during this period when
486 examined across the entire sample (Pearson's r = 0.12 and 0.21, p = 0.25 and 0.046 for the left and
487 right hemispheres, respectively; Figure 4B). Conversely, PSC in either convergent hemisphere
488 during perturbation was not associated with objective measures of physiological arousal (*i.e.,* mean

change in heart rate, Pearson's r = 0.11 and 0.09, p = 0.31 and 0.40 for left and right hemispheres, respectively), post-scan ratings of cardiac intensity (Pearson's r = 0.16 and 0.20, p = 0.15 and 0.06), post-scan ratings of respiratory intensity (Pearson's r = 0.12 and 0.06, p = 0.26 and 0.58 for left and right hemispheres, respectively), post-scan ratings of state anxiety (Pearson's r = 0.14 and 0.08, p = 0.20 and 0.49 for left and right hemispheres, respectively), or trait measures of anxiety sensitivity (*i.e.,* ASI-Total, Pearson's r = 0.12 and 0.16, p = 0.25 and 0.13 for left and right hemispheres, respectively).

Finally, pre- to post-task resting state functional connectivity of the convergent regions showed a pattern of differential change in the ADE compared to HC group: functional connectivity between the right dysgranular convergent cluster and left middle frontal gyrus increased in the ADE group only, while the HC group saw no differences ($p < 0.05$, corrected; Figure 5A and 5B). This was the only significant cluster showing connectivity differences between groups. When looking at this insular-IFG connection across the entire sample, the magnitude of functional connectivity change between these two areas was associated with trait anxiety (Pearson's r = 0.43 and 0.36 for OASIS and GAD7, respectively, $p < 0.001$) and trait depression (Pearson's r = 0.38, $p < 0.001$ for PHQ-9) (Figure 5C) but not the magnitude of ISO-induced heart rate (Pearson's r = -0.05, p = 0.66) or dial rating (Pearson's r = 0.01, p = 0.90) at the 2.0μg dose.

Divergence analysis

The Anticipation period of the ISO task engaged large swaths of the bilateral agranular insular cortex that were not activated at any point during the VIA task (Figure 6A) (Table 3). During this period, the right hemisphere was activated to a greater spatial extent than the left in both groups (χ^2_1 = 22.7 and 7.3, $p < 0.001$ and p=0.007 for left vs. right in the HC and ADE groups, respectively), and to a greater spatial extent in HC versus ADE individuals in the right hemisphere only (χ^2_1 = 7.3, p=0.007 for group comparison). There was no group difference in the spatial extent in the left hemisphere (χ^2_1 = 2.0, p = 0.15) (Figure 6B). Notably, these spatial patterns of activation were similar between groups (Dice coefficient =0.86 in the left and 0.87 in the right).

During the Peak period of the Saline dose, the spatial extent of activation in the agranular insula increased to include significantly more voxels, for both groups and hemispheres (χ^2_1 = 75.3 and 71.4, $p < 0.001$ for Anticipation vs. Peak in the left and right hemispheres in HC; χ^2_1 = 36.3 and 12.1, $p < 0.001$ for Anticipation vs. Peak in the left and right hemispheres in ADE) (Figure 6B). This activation expansion occurred to a greater degree in the HC versus ADE group (χ^2_1 = 17.2 and 70.3, corrected $p<0.001$ for HC versus ADE in the left and right hemispheres, respectively). Finally, agranular insula recruitment within the HC group during the Saline Peak period was shifted towards the right hemisphere (*i.e.*, more active voxels in the right than the left, χ^2_1 = 24.3, $p < 0.001$), while the ADE group showed no hemispheric difference during this period (χ^2_1 = 0.10, p = 0.75). Despite this difference in number of activated voxels, the spatial patterns of activation were still largely overlapping between groups (Dice coefficient = 0.88 in the left, 0.82 in the right).

Along with expansions in the spatial extent of activation, the signal intensity in the agranular insula increased from the Anticipation period to the Saline Peak period ($F_{1,270}$=28, $p<0.0001$ for main effect of epoch), with no differences between groups ($F_{1,270}$ = 0.25,p = 0.62 for the main effects of group) (Figure 6C). This increase occurred in both hemispheres (t_{270} = 2.7 and 4.8, p = 0.008 and < 0.001 for Saline Peak – Anticipation contrast in the left and right hemispheres,

respectively, when collapsed across groups). Notably, the right hemisphere was activated more strongly than the left during the Saline Peak period (t_{270} = -3.0, p = 0.003), whereas there was no difference across hemispheres in the Anticipation period (t_{270} = -0.8, p = 0.41). The magnitude of agranular insula activation was not related to trait measures of anxiety sensitivity in either epoch or hemisphere when examined transdiagnostically across groups (ASI * hemispheric interaction effect: $F_{1,90}$ = 1.9, p = 0.17 for Anticipation, and $F_{1,90}$ = 1.7, p = 0.19 for Saline Peak).

Physiological response and perceptual ratings

During the 2.0mcg dose there were large perturbations in heart rate in both groups, and while the ADE appeared to have a slightly greater response on average, this reached statistical significance via permutation testing only during two continuous time points in the Peak period (seconds 98 through 99, t = 1.7 and 1.5, p = 0.044 and 0.045, Figure 7A). However, the ADE group reported significantly higher real-time dial ratings for the latter portion of the Peak period extending into much of the ensuing recovery period (seconds 110 through 142, t = 1.8–2.3, p = 0.008–0.042, Figure 7B). During the Saline dose of the ISO task, both heart rate and perceptual dial ratings remained near baseline levels. While heart rate did not differ between groups (t = -0.53 – 1.64, p = 0.05 – 1.00), the HC group showed small but statistically significant increases in dial ratings compared to those of the ADE group for portions of the Peak period and the ensuing recovery period (t = -1.67 – -2.60, p = 0.005 – 0.048) (Figure 7A and 7B). Although there were ISO-induced differences in continuous measures of cardiorespiratory sensation, there were no group differences in retrospective cardiac or respiratory intensity ratings for the 2.0 mcg infusion (t_{80} = 1.5 and 1.2 for heart and lungs respectively, p = 0.13 and 0.25) or the saline infusion (t_{80} = 0.3 and 1.2, p = 0.75 and 0.22) (Figure 7C). The ADE group reported greater retrospective anxiety than the HC group following infusions (t_{85} = 4.8 and 3.8 for 2.0mcg and Saline, respectively, p < 0.001), with no differences in excitement (t_{85} = 0.2 and 0.9, p = 0.80 and 0.37 for 2.0mcg and Saline, respectively). During the VIA task, the ADE group reported higher cardiac intensity ratings than the HC group during heart-focused attention (t_{89} = 2.0, p = 0.04) but lower exteroceptive intensity ratings during the target condition (t_{90} = 2.7, p < 0.01). There were no group differences in the intensity of reported lung or stomach sensations (t_{89} = 1.6 and 1.4, p = 0.10 and 0.16) (Figure 7D).

Discussion

The current study revealed overlapping patterns of neural activation within the dysgranular mid-insula during top-down and bottom-up interoceptive processing, corroborating previous studies examining each task independently (Hassanpour et al. 2018, Simmons et al. 2013), and supporting the notion of the insula as a key functional interface between goal-directed and sensory-driven interoceptive streams. Importantly, hemispheric differences in the patterns of dysgranular activation distinguished individuals with anxiety, depression, and eating disorders from healthy comparisons, as hypothesized. These hemispheric asymmetries, and the disparate spatial patterns within the left dysgranular insula, support the conceptualization of this subregion as a “locus of disruption” for interoceptive symptomatology in these disorders (Nord et al. 2021). The hemispheric imbalance was concurrent with a heightened perceptual response in the clinical sample, as well as with changes in right dysgranular insula-to-left middle frontal gyrus functional

connectivity following the interoceptive tasks. Finally, activity within the agranular insula was selective to periods of increased interoceptive expectancies, aligning with a prediction-generating role for this region and one that was distinct from the convergent effects seen in the dysgranular mid-insular subregion.

Top-down processing commonly refers to cognitive influences on perception, such as attention, memory, and expectation, that putatively help the brain to make sense of the stimuli it encounters. In contrast, bottom-up processing commonly refers to the stimulus-driven signals that are processed hierarchically as they reach the brain. With respect to interoception, top-down processing can refer to the brain's ability to predict or interpret how the internal body should feel (*i.e.,* the expected interoceptive signals) based on the previous or current environmental context. In turn, bottom-up processing can refer to the actual state of the body in the current moment. For instance, top-down influences may include the anticipation of an upcoming meal leading to feelings of hunger, while bottom-up influences may refer to actual hunger signals from the body at lunch time, such as hormonal concentrations of ghrelin/leptin, and stomach contractions. The continuous balance between these processes determines the qualia of conscious perceptions and has been suggested to be key to health and the optimization of internal and subjective states (Sterling 2012). However, as processes, they are rarely studied concomitantly in the manner conducted in this study. The convergence identified between top-down and bottom-up interoceptive processing within the dysgranular mid-insula suggests that this cortical subregion is an area where further detail regarding the reciprocal interactions underpinning interoceptive perceptions should be investigated, particularly in relation to psychiatric disorders involving disturbances of mood, anxiety, or appetite.

Although the current findings emphasize the role of interoceptive processing within dysgranular subregions of the insula, a number of experimental and analytic next steps are worth considering. Due to the broad systems-level of inference allowed by fMRI methodology and the relatively rudimentary block averaging analytic approach employed, additional measurements are warranted to establish the cellular and molecular mechanisms underlying the observed dysgranular co-activation. Such approaches would be important for verifying a true intersection of interoceptive neurocircuitry in which connecting top-down attention and prediction circuits directly modulate, or are modulated by, incoming sensory afferences. An alternative outcome could be identifying an overpassing flow of signals across these circuits within the same region. Implementing high resolution approaches to imaging these processes via high-field fMRI on a trial-by-trial basis could inform the laminar architecture underpinning attention-driven modulation of incoming viscerosensory signals as well as allowing for computational modelling of these processes at the level of cortical laminar subfields (Kasper et al. 2022). In an interoceptive application of this analyses employing a respiratory bottom-up perturbation approach, activation of the anterior insula was associated with the prediction certainty but not prediction error for different inspiratory breathing loads, with parameters distinguishing between high versus low trait anxiety individuals (Harrison et al. 2021). This computational approach could be adapted for cardiorespiratory processing within the dysgranular insula. While typically restricted to high field strengths, such as 7 Tesla, there are emerging reports that laminar imaging can be performed at lower field strengths (Knudsen et al. 2023). Thus, there are a number of currently feasible steps for further extending the present findings.

While we did not set out to test predictive coding or other computational models in the current study, certain computationally relevant theories provide useful frameworks for interpreting the observed dysgranular co-activation during each imaging task. These include the

620 Embodied Predictive Interoceptive Coding (EPIC) model (Barrett and Simmons 2015), describing
621 laminar-specific hypotheses for the interactions between anterior-mediated interoceptive
622 predictions and posterior-mediated viscerosensation across the antero-posterior axis of the insula,
623 and the Insula Hierarchical Modular Adaptive Interoception Control model (Fermin et al. 2022)
624 using the hierarchical tripartite subdivision of the insula and describing parallel networks within
625 prefrontal cortical and striatal regions that underpin higher-order interoceptive representation. For
626 additional theoretical discussions of the computational functional neuroanatomy of interoception,
627 see Allen et al. (2022), Paulus, Feinstein, and Khalsa (2019), and Petzschner et al. (2021).
628 Collectively, these theories can be interpreted to suggest a model of bidirectional signal flow along
629 the antero-posterior axis of the insula: while the granular posterior subregions may be the first to
630 receive ascending visceral input, the agranular anterior subregions continuously issue predictions
631 regarding the anticipated states of such input (Barrett and Simmons 2015). From this perspective,
632 the dysgranular mid-insula is well-positioned between the agranular and granular poles to
633 integrate the signals from each source. Computations within dysgranular layers can link incoming
634 sensations with top-down expectations (as suggested in the EPIC model), effectively translating
635 visceral signals into endogenously meaningful interoceptive prediction error signals, and providing
636 the rest of the brain with an internal context for interpreting the current bodily state (Seth and
637 Friston 2016).
638 Applying computational frameworks for interoception to the present findings may also be
639 useful for interpreting the broad agranular insula activation found only during periods of increased
640 bodily expectancies (*i.e.*, "divergence"). This subregion's engagement during the Anticipation
641 window and expansion throughout the Peak period of the Saline dose likely reflects an increase in
642 predictive processing during these conditions, as both groups expected a potential perturbation
643 and were subsequently required to update their predictions upon experiencing a physiologically
644 quiescent state instead. The reduced spatial extent of this activation in the ADE versus HC group
645 could plausibly stem from an overreliance on top-down predictions and perhaps a pruning of
646 spatial activation in the associated regions, similar to the functional alterations of neural activity
647 that have been observed following the acquisition of a motor skill (Wiestler and Diedrichsen 2013).
648 Such 'efficient' neural exchanges might even result from a chronic inability to adjust confidence in
649 bodily input in relation to its ambiguity (*i.e.,* increasing confidence in visceral signals during bodily
650 perturbation), and could occur alongside maladaptive allostatic interoceptive adjustments
651 described in psychiatric disorders (Barrett, Quigley, and Hamilton 2016; Smith et al. 2020).
652 Computational theories of interoception can also be applied to the observed co-activation within
653 the dysgranular mid-insula (i.e., "convergence"). Dysgranular convergence aligns with our proposed
654 intersectional (as opposed to overpassing) role for signal processing this region, and could
655 represent the generation of prediction errors as inflows of isoproterenol-induced viscerosensation
656 are compared to task-specific interoceptive predictions focused by the lens of directed attention.
657 While internally-directed attention alone might selectively enhance cortical representations of the
658 viscera across wide swaths of insula, as suggested previously (Avery et al. 2014; Pollatos et al.
659 2007), these past studies focus narrowly on perceptions of the viscera during physiological
660 quiescent states when visceral signals are relatively ambiguous. By manipulating cardiorespiratory
661 signals during the ISO 2.0mcg dose and eliciting unambiguous perceptual states, the current study
662 effectively spotlights the dysgranular subregion's role in heightened interoceptive awareness and

provides a neuroanatomical focus for further examinations of bi-directional interoceptive processing in this important region.

The right-hemispheric increase in mid-insula activity, as well as the hemispheric asymmetries and altered functional connectivity found in the ADE group has several implications for an interoceptive processing role for the dysgranular insula. Previous authors have suggested a right-hemispheric dominance in interoceptive processing in healthy populations (Craig 2009; Schulz 2016), and have pointed towards the right anterior insula as the key hub for body awareness (Craig 2009). While a rightward emphasis in the magnitude of insular activation was found during ISO-induced cardiorespiratory sensations across both groups, this activity was located more posteriorly, towards the mid insula (similar to previous isoproterenol fMRI studies (Hassanpour et al. 2016, 2018)), where it was correlated with cardiorespiratory sensation. While this finding supports a role for the mid-insula as an integrative hub for interoceptive awareness, it was in contrast to a lack of clear associations with physiological signals, emotional feelings such as anxiety or excitement or trait measures of ADE severity, despite the evocation of greater state anxiety following perturbation in the ADE individuals. Probing the symptomatic relevance these potential brain-behaviour relationships may call for more refined approaches to the study of interoceptive perturbation. One option might be to evaluate the intersecting influence of several forms of perturbation, by studying both exogenous approaches such as isoproterenol infusion, and endogenous approaches such as mental stressors (i.e., Stroop task (Gianaros et al. 2005)), physical stressors (i.e., Valsalva (Song et al. 2018) or lower body negative pressure (Kimmerly et al. 2005)), or social stressors (i.e., Trier Social Stress task (Allen et al. 2017)) within the same individuals.

Despite observing several right hemispheric associations across both groups, the ADE group demonstrated a clear leftward activation asymmetry and distinct activation patterns in the left dysgranular mid-insula across both the ISO and VIA tasks. These left insula abnormalities are compatible with the "locus of disruption" identified by Nord et al. (2021), when conducting an fMRI meta-analysis of existing top-down or bottom-up interoception studies of various psychiatric populations. However, beyond identifying a plausible region of cortex, the precise mechanisms underlying this disruption remain unclear. Assuming an intersectional role involving intermingling of top-down and bottom-up streams, it seems plausible that numerous mechanisms could contribute to the aberrant processing identified in the current study. Such mechanisms include a reduced attentional enhancement of ascending visceral input (Avery et al. 2014; Kerr et al. 2016), and/or an inflexibility in adjusting to the salience of interoceptive signals occurring during perturbation, as revealed by computational modeling (Smith et al. 2020). Reduced flexibility of neural processing may also explain the singular finding of altered connectivity between the right mid-insula and left middle frontal gyrus following the interoceptive tasks in the ADE group, as this frontal region is likely involved in in attentional control including attention bias to threat or internal representations (Henseler et al. 2011; Sylvester et al. 2003; White et al. 2016). An inability to return this coupling to baseline following interoceptive engagement (or a shift in the opposing direction than HCs) could suggest a dysregulated attentional switching mechanism, particularly since the degree of connectivity change was associated with trait measures of anxiety and depression severity.

From an affective standpoint, the observed hemispheric divergence in interoceptive processing is worth considering in the context of the functional lateralization of emotion theories

proposed within the insula. Such theories (Craig, 2005; Davidson et al., 1999, 2004; Picard et al., 2016), supported by meta-analytic (Murphy, Nimmo-Smith, and Lawrence 2003) and human brain stimulation Oppenheimer et al. 1992) findings, have attributed the left anterior insula to the energy-enriching behaviors of the parasympathetic nervous system, and the right anterior insula with the energy-expending ones of the sympathetic nervous system (Oppenheimer et al. 1992). The current finding of right-hemispheric dominance for conscious awareness of isoproterenol (an arousal-like, and thus sympathetic-emulating manipulation), as well as the increased signal intensity in the right anterior insula during the expectancy of such manipulation, may be considered aligned with this perspective. Correspondingly, activity within the right insula has been associated with conscious awareness of threat (Critchley, Mathias, and Dolan 2002), and mouse models have shown causal evidence for the right anterior insula in orchestrating stress responses to aversive visceral stimuli (Wu et al. 2020). However, assumptions of autonomic opponency are likely overly simplistic, and it is more appropriate to consider these systems as functionally coupled across spinal and vagal systems instead of anatomically distinct (Jänig 2006; Jänig et al. 2017). In this manner, an admittedly speculative emotional lateralization account of functional coupling might posit that the right anterior insula generates interoceptive predictions of spinal efference and the left anterior insula for those of vagal efference; in turn the respective dysgranular areas would then be specialized towards receiving and computing the prediction errors of these different inputs. However, since there does not appear to be an neuroanatomical lateralization for afferent tracts (*i.e.,* spinal input does not have a preference for the right hemisphere, and vagal not for the left) (Dum, Levinthal, and Strick 2009; Shipley and Sanders 1982), it seems more plausible that the contribution of interoceptive processing to emotion requires a carefully integrated balance of both autonomic systems across both hemispheres. Based on the present data, such a balance appears to be asymmetrically shifted in the setting of psychiatric disorders affecting the anxiety, depression, and disordered eating spectrums, particularly during modulations of interoceptive state.

There are several limitations and strengths of the present approach to consider. First, while the quantification of insula asymmetries was strengthened by the use of previously established task-specific pipelines and justified by cytoarchitectural hypotheses leveraging prominent theories about interoceptive neurocircuitry, several analysis steps differed between the tasks that could impact the observed results, including the use of a block versus event-related design and differences in the regression of physiological noise and motion correction. This pre-specified approach was intentional. It allowed confidence that the analysis metrics were sound (i.e., that a voxel counted as co-activated would have good task-validity in relation to the methods of previously published ISO and VIA studies). However, it also meant that there was variability within-individuals in how the data was handled for each task. Future approaches involving harmonized pre-processing steps across both tasks may be considered. Second, the present approach to determining 'convergence' was admittedly simplistic in relying on co-activation as a determinant. Applying more sophisticated analysis techniques, such as those amenable to individual-level pattern analyses (as opposed to group activation maps) would provide greater insight into the individual responses of each participant. Such approaches are worth considering as they are a core component of personalized evaluations applying functional neuroimaging to diagnostic validation or treatment selection (Goldstein-Piekarski et al. 2022). Third, while the use of tripartite insular subregions was appropriate to the level of resolution in our data, future investigations could

749 employ high resolution fMRI to directly test the laminar-specific hypotheses of the predictive
750 coding theories we have discussed. Fourth, while the conceptual approach to the top-
751 down/bottom-up construct may mask the complexity of the brain (Rauss and Pourtois 2013) and
752 the process of attention (Hommel et al. 2019), the integration of this concept with several
753 behaviorally relevant tasks in the same individuals offers a useful and informative heuristic in its
754 application. Finally, while our results focus on the insula's role in cardiorespiratory awareness, it's
755 important to note that the insula isn't the only brain area involved in sensing internal body states
756 (Berntson and Khalsa 2021; Mayeli et al. 2023). Future research should explore structural and
757 functional relationships between the insula and the rest of the brain; for example, relationships
758 between white matter tracts (Ghaziri et al. 2017, 2018), grey matter volume (Hatton et al. 2012) ,
759 and functional coupling (Cauda et al. 2011). To build this more complete picture of interoceptive
760 processing, other sophisticated network-based and whole-brain analysis approaches will be
761 required, including those oriented towards the development of clinically-predictive models for
762 interoceptive symptoms in psychiatric disorders.
763

764 **Conclusion**

765 This study confirms the pivotal role of the dysgranular insula in the processing of top-down
766 and bottom-up interoceptive inputs, and validates the dysgranular mid-insula as a possible locus of
767 interoceptive disruption in psychiatric disorders.

768

769 **Funding:**

770 National Institute of Mental Health NIMH K23MH112949, R01MH127225 (to SSK) and National
771 Institute of General Medical Sciences NIGMS 1P20GM121312 (to SSK).
772
773

774 **Disclosures/competing interest:**

775 The authors have no financial or non-financial competing interests to disclose.
776
777

778 **Acknowledgements**:

779 The authors would like to thank Maria Puhl and Gabriel Morrison for their contributions to data
780 preprocessing, as well as Valerie Upshaw and Rachel Lapidus for their assistance with data
781 collection.
782
783

Figures and Tables

Table 1. Demographic information for the transdiagnostic anxiety, depression, and/or eating disorders (ADE) group and the propensity-matched healthy comparison (HC) group. GAD = generalized anxiety disorder, MDD = major depressive disorder, AN = anorexia nervosa, PTSD = post-traumatic stress disorder, OCD = obsessive compulsive disorder, SUD = substance use disorder, BMI = body mass index, STAI = State-Trait Anxiety Inventory, ASI = Anxiety Sensitivity Index, with a Total Score, and Physical, Cognitive, and Social subscales, PHQ-9 = depression module of the Patient Health Questionnaire, SCOFF = "Sick, Control, One, Fat, Food" eating disorder questionnaire.

	HC (n=46)	ADE (n=46)	t	df	p-value
Sex	41 Female 5 Male	45 Female 1 Male	-	-	-
Age	24 (5)	25 (7)	0.57	80.49	0.57
BMI	23.48 (3.26)	23.34 (3.33)	-0.20	89.97	0.84
STAI	30.0 (1.1)	56.0 (1.4)	-14.43	83.01	**<0.0001**
ASI-Total	7.39 (5.26)	13.98 (8.89)	8.89	57.47	**<0.0001**
ASI-Physical	1.15 (1.59)	5.19 (5.81)	5.81	53.38	**<0.0001**
ASI-Cognitive	0.98 (1.47)	7.41 (6.53)	6.52	49.54	**<0.0001**
ASI-Social	5.26 (4.04)	13.83 (6.08)	7.96	78.28	**<0.0001**
PHQ-9	0.78 (1.11)	10.39 (5.98	10.72	48.12	**<0.0001**
SCOFF	0 (0)	1.09 (1.23)	6.01	45	**<0.0001**
Diagnoses	No psychiatric disorders	67% GAD 72% MDD (current or remitted) 35% AN 13% Social anxiety disorder 11% PTSD 4% OCD 4% SUD	-	-	-
Medication use	None	*Taking one or more psychiatric medication:* Serotonergic[1]: 35% Histaminergic[2]: 11% Dopaminergic[3]: 7% SNRI[4]: 7% Benzodiazepene[5]: 4% Miscellaneous[6]: 2% Beta-blocker[7]: 2%	-	-	-

[1]*Escitalopram, Fluoxetine, Trazodone, Sertraline, Paroxetine, Duloxetine*
[2]*Lamotrigine, Hydroxyzine, Doxepin*

[3]*Olanzapine, Aripiprazole, Quetiapine*
[4]*Atomoxetine, Buproprion, Desvenlafaxine*
[5]*Clonazepam, Alprazolam*
[6]*Vortioxetine*
[7]*Propranolol*

807 **Table 2.** Insular regions demonstrating convergent processing between top-down and bottom-up
808 interoception**.**

	MNI coordinates (center of mass)			Volume (mm^3)
	X	*Y*	*Z*	
Left Insula: ADE	-39	-0.1	-8.2	1736 (217 voxels)
Left Insula: HC	-40	-1.3	-4.8	1240 (155 voxels)
Right Insula: ADE	39	2.3	-12.9	1088 (136 voxels)
Right Insula: HC	39.9	2.2	-10.3	1960 (245 voxels)

809

810

811

812 **Table 3.** Agranular anterior insular regions demonstrating divergent processing during periods of
813 increased bodily expectancies.

		MNI coordinates (center of mass)			Volume (mm^3)
		X	*Y*	*Z*	
Anticipation	**Left: ADE**	-31.6 -31.9	17.9 9.2	4.8 -15	1168 (146 voxels) 344 (43 voxels)
	Left: HC	-31.5	15.2	-1.2	1688 (211 voxels)
	Right: ADE	35.4	19.1	1.4	1648 (206 voxels)
	Right: HC	37 35	13 7	-9 -19	1744 (218 voxels) 368 (46 voxels)
Saline (Peak)	**Left: ADE**	-33.1	16.7	-1.6	2264 (283 voxels)
	Left: HC	-33.2	15.7	-2.7	2760 (345 voxels)
	Right: ADE	35.4	18.6	-0.9	2120 (265 voxels)
	Right: HC	34.3	16.7	-4.7	3024 (378 voxels)

814

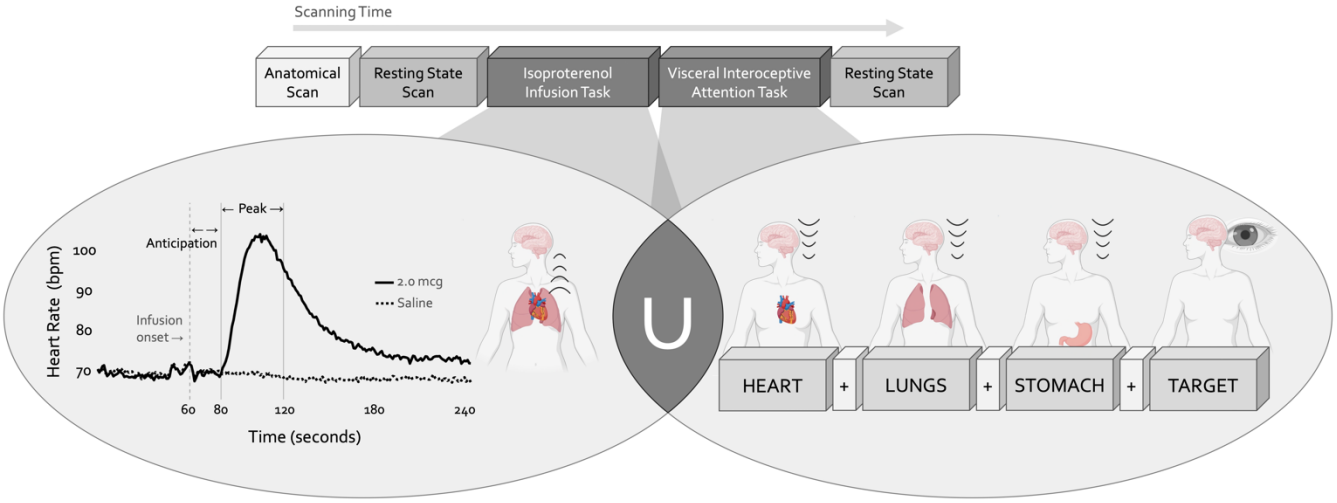

Figure 1. Experimental design. During a single functional neuroimaging scanning session two neuroimaging tasks were used to localize the convergence between bottom-up and top-down interoceptive processing. The Isoproterenol Infusion (ISO) task manipulated interoceptive input in a bottom-up manner, while the Visceral Interoceptive Attention (VIA) task manipulated interoceptive attention in a top-down manner. During the ISO task, participants were asked to attend to their cardiorespiratory sensations while receiving double-blinded infusions of either isoproterenol 2.0 micrograms (mcg, solid line) or 0.5mcg (not pictured), a rapidly acting peripheral beta-adrenergic analogue eliciting transiently increased cardiovascular and respiratory signals in a manner akin to adrenaline, or infusions of saline (dashed line), resulting in no physiological change. During the VIA task, on-screen cues directed participants to shift their attention towards naturally occurring body sensations from a particular internal organ (heart, lungs, or stomach, the interoceptive attention conditions) or the word "TARGET" (the exteroceptive attention condition) that would flash at different intensities. No infusions were given during this task, so the body remained at physiological rest. Both tasks were preceded and followed by a resting state scan.

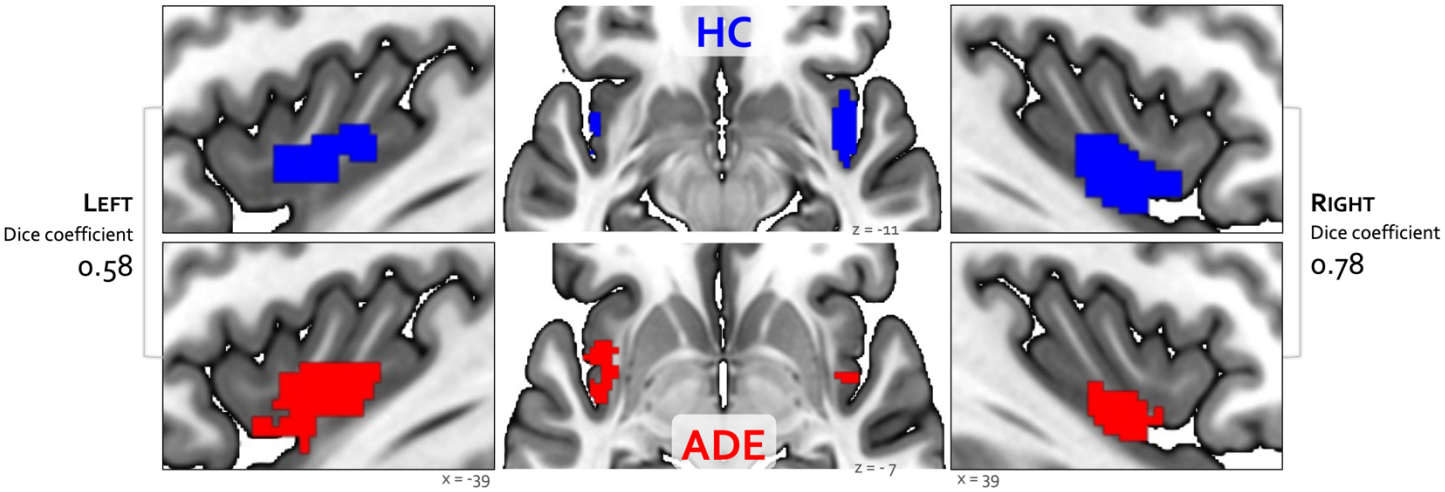

Figure 2. Convergence between bottom-up and top-down interoceptive processing in healthy comparisons (HC, top row) and individuals with anxiety, depression, and/or eating disorders (ADE, bottom row). Each convergence map reflects the only cluster of voxels that were co-activated across the whole brain during the ISO task, involving perturbation of cardiorespiratory signals, and the VIA task, involving goal-directed interoceptive attention towards cardiac and respiratory signals at rest. Numbers on the left and right reflect the Dice similarity coefficient, which are used to quantify the degree of spatial overlap between groups. Relative to HCs, the ADE group showed lower spatial similarity for the left insular cortex (Dice coefficient of 0.58), than the right insular cortex (Dice coefficient of 0.78).

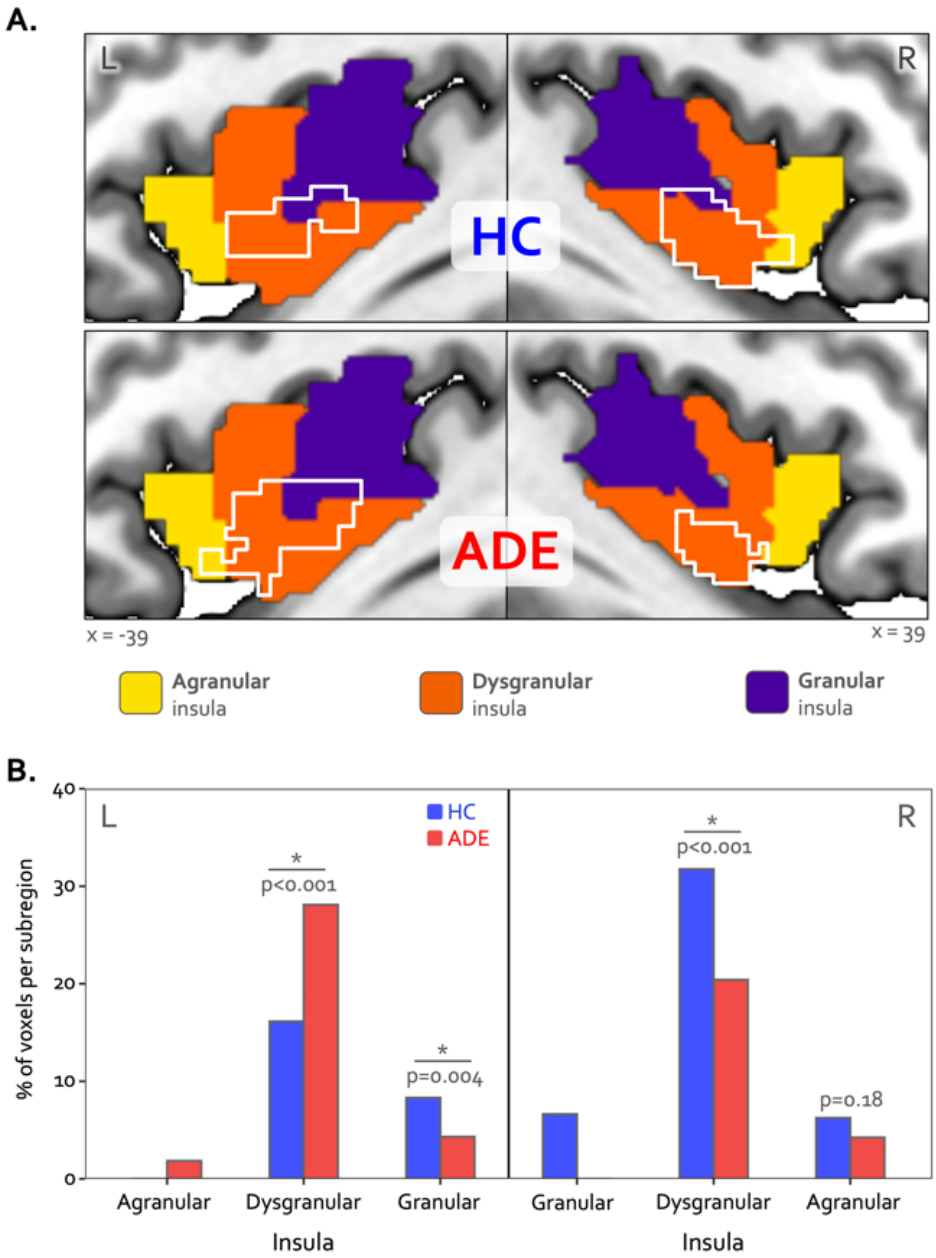

Figure 3. Hemispheric divergence of bottom-up and top-down interoceptive processing across psychiatric disorders. (A) Hemisphere-specific convergence maps (white outlines) overlaid on a tripartite probabilistic cytoarchitectonic division of the insular cortex. (B) Quantification of convergence within each cytoarchitectonic subregion (*i.e.,* number of co-activated voxels in relation to the total number of voxels within that subregion), showing asymmetric proportional voxel co-activation in the left and right dysgranular insula between the groups. *indicates significant group difference for the proportion of co-activated voxels in each subregion via chi-square test. HC: healthy comparison. ADE: anxiety, depression, and/or eating disorder.

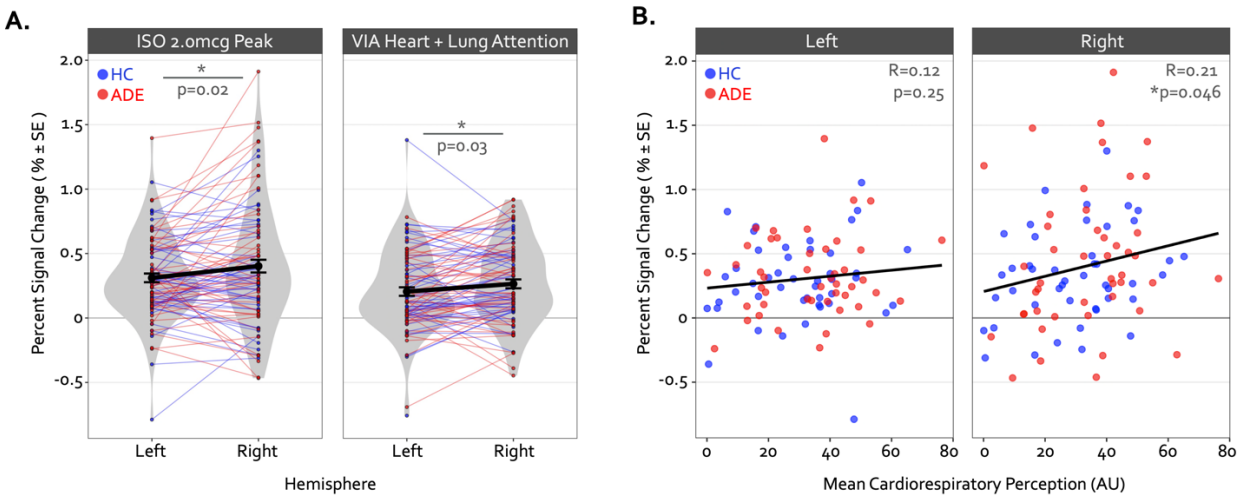

Figure 4. Hemispheric differences in the activation magnitude of the convergent dysgranular insula subregion. (A) Co-activated voxels within the right dysgranular insula subregion exhibited a greater degree of percent signal change during the Peak period of the 2.0mcg dose in the ISO task (left sub panel) and during the Heart and Lung attention condition in the VIA task (right sub panel). As there were no main effects of group, mean percent signal change is collapsed across groups. *indicates $p<0.05$ for the left versus right post-hoc contrast, following a main effect of hemisphere in the linear mixed effects regression. (B) Across both groups the mean percent signal change within the right but not left convergent dysgranular insula subregion was correlated with real-time cardiorespiratory intensity ratings during the Peak period of the 2.0mcg dose in the ISO task. *indicates $p<0.05$ for the Pearson's R correlation coefficient, separately for each hemisphere.

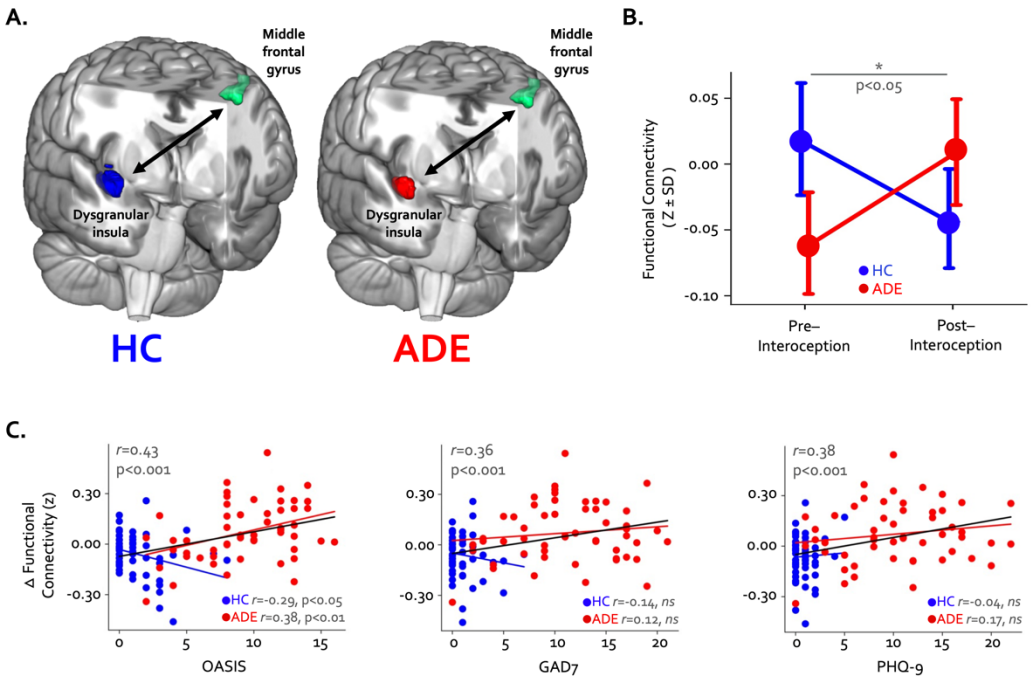

Figure 5. Changes in whole-brain functional connectivity of convergent dysgranular insula subregions following performance of the interoceptive tasks. (A) Functional connectivity between the right convergent dysgranular insula subregion and the left middle frontal gyrus showed opposing effects in the ADE versus HC groups. (B) While functional connectivity between these regions increased from baseline following interoception in the ADE group, it decreased in the HC group, resulting in a significant interaction effect. (C) Across the entire sample changes in functional connectivity were associated with trait measures of anxiety and depression. When examined in each group individually, associations between connectivity change and trait anxiety occurred in opposite directions (left and middle panel).

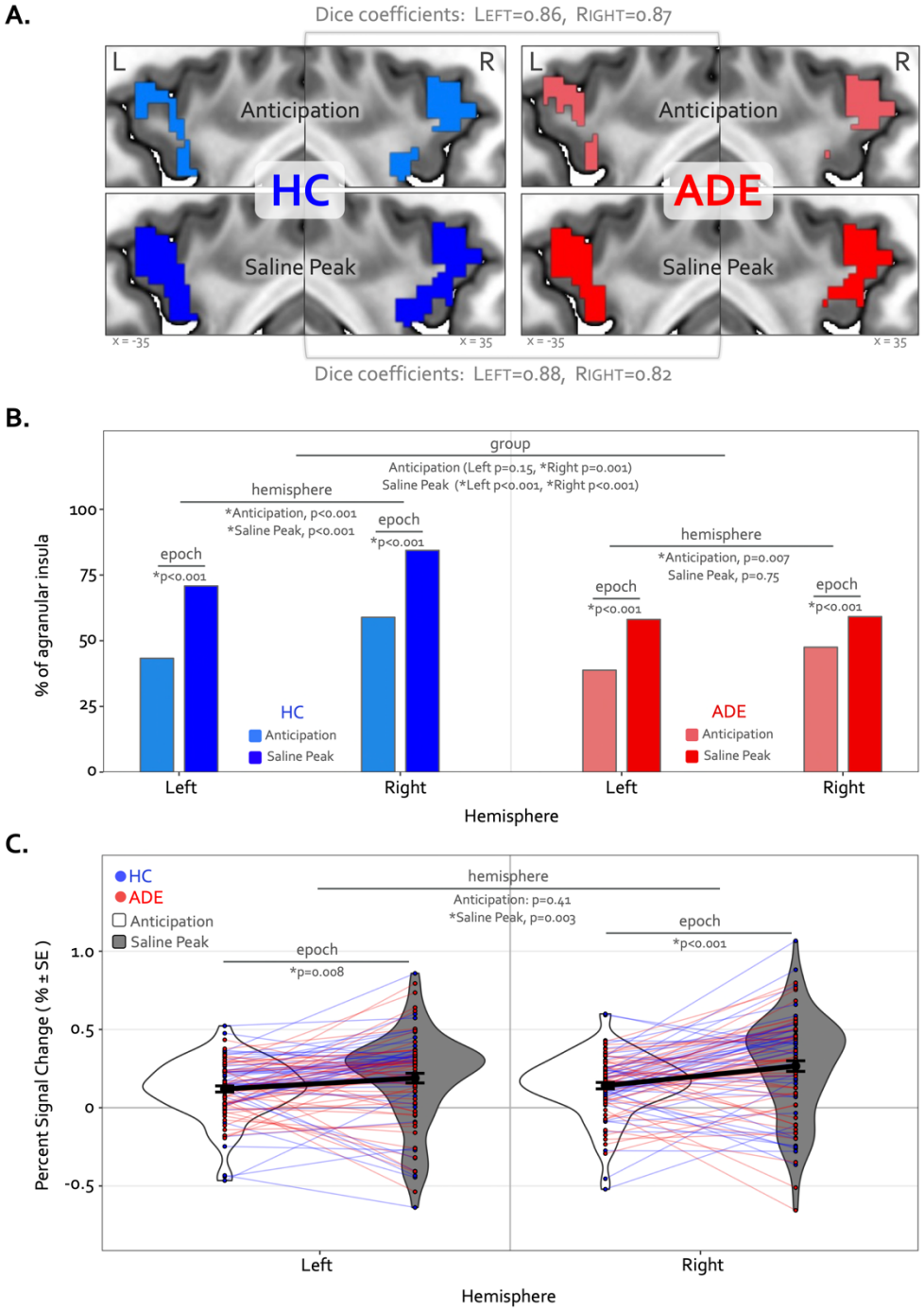

Figure 6. Divergence of top-down processing during interoceptive uncertainty in individuals with anxiety, depression, and/or eating disorders (ADE) and healthy comparisons (HC). (A) Selective activation of the bilateral agranular anterior insula during the Anticipation period (top) and Saline Peak period (bottom) of the ISO task. Both epochs demarcate periods of maximal expectancy about future changes in body state while the body remains at physiological rest (i.e., no ensuring evidence of heart rate or breathing rate increases). These brain areas showed activity only during these

885 periods of the ISO task and were not active during the Heart and Lung attention part of the VIA task,
886 indicated they have specialized roles. (B) Quantifying the spatial extent of this agranular activation
887 (*i.e.,* number of active voxels in relation to total number of voxels in that subregion) revealed that
888 greater right hemisphere activation during the anticipation window occurred for both groups, and
889 more so in the HC than the ADE group. During the peak period of Saline this activation covered
890 more of the bilateral agranular insula in both groups. However, the right hemisphere was activated
891 more than the left in both groups, and the HC group exhibited more active voxels in the right
892 hemisphere than the left, and more than the ADE group in both hemispheres, while the ADE group
893 showed no hemispheric difference during this window. (C) Increased ISO-specific activation of
894 agranular insular during the anticipation period versus the saline peak period. This pattern,
895 occurring for both hemispheres and across both groups, was greater in the right than the left
896 hemisphere.
897

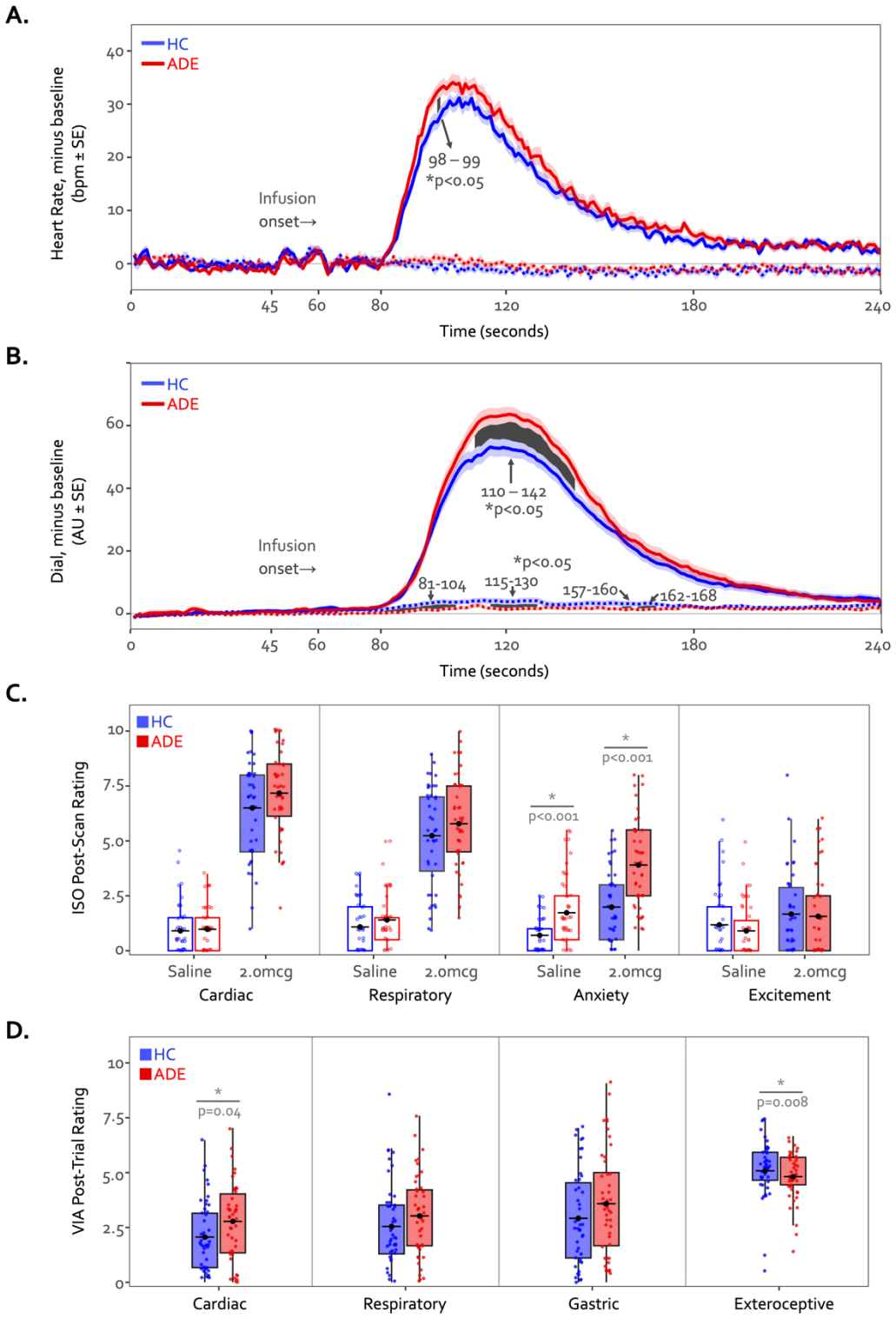

Figure 7. Time courses of heart rate (A) and continuous dial ratings (B) during the 2.0mcg (solid lines) and Saline (dotted lines) doses of the ISO task. Heart rate changes observed during both infusions were generally similar between both groups across the majority of the infusion period.

The cluster-based permutation analysis showed a two-second instance of significantly higher heart rate in the ADE group starting at the 98th second of the 2.0mcg dose only during the Peak period, followed by a prolonged increased in dial rating for large portions of the Peak and Recovery periods (seconds 110 through 142, shown via the shaded area). No heart rate differences were observed during the Saline infusion. *indicates $p<0.05$ for significant group difference using permutation analysis. (C) Retrospective ratings on the ISO task showed no significant group differences in cardiac or respiratory intensity or excitement following saline or the 2.0mcg infusion, while the ADE group reported increased anxiety following both infusions. (D) Sensation ratings during the VIA task. The ADE group reported higher cardiac intensity ratings than the HC group but lower exteroceptive ratings, with no group difference in respiratory or gastric sensation ratings. *indicates $p<0.05$ for two-sample t-test between groups, separately for each condition. Where appropriate, both the p-value and Cohen's d are shown.

References

Adamic, Emily, Jason Avery, Sahib S. Khalsa, and Adam Robert Teed. 2021. "Convergence between Goal-Directed and Stimulus-Driven Streams of Cardiorespiratory Interoception." doi: 10.17605/OSF.IO/6NXA3.

Adolfi, Federico, Blas Couto, Fabian Richter, Jean Decety, Jessica Lopez, Mariano Sigman, Facundo Manes, and Agustín Ibáñez. 2017. "Convergence of Interoception, Emotion, and Social Cognition: A Twofold FMRI Meta-Analysis and Lesion Approach." *Cortex* 88:124–42. doi: 10.1016/j.cortex.2016.12.019.

Allen, Micah, Andrew Levy, Thomas Parr, and Karl J. Friston. 2022. "In the Body's Eye: The Computational Anatomy of Interoceptive Inference." *PLoS Computational Biology* 18(9):e1010490. doi: 10.1371/journal.pcbi.1010490.

Augustine, J. R. 1996. "Circuitry and Functional Aspects of the Insular Lobe in Primates Including Humans." *Brain Research. Brain Research Reviews* 22(3):229–44. doi: 10.1016/s0165-0173(96)00011-2.

Avery, Jason A., Kaiping Burrows, Kara L. Kerr, Jerzy Bodurka, Sahib S. Khalsa, Martin P. Paulus, and W. Kyle Simmons. 2017. "How the Brain Wants What the Body Needs: The Neural Basis of Positive Alliesthesia." *Neuropsychopharmacology* 42(4):822–30. doi: 10.1038/npp.2016.128.

Avery, Jason A., Wayne C. Drevets, Scott E. Moseman, Jerzy Bodurka, Joel C. Barcalow, and W. Kyle Simmons. 2014. "Major Depressive Disorder Is Associated with Abnormal Interoceptive Activity and Functional Connectivity in the Insula." *Biological Psychiatry* 76(3):258–66. doi: 10.1016/j.biopsych.2013.11.027.

Barrett, Lisa Feldman, Karen S. Quigley, and Paul Hamilton. 2016. "An Active Inference Theory of Allostasis and Interoception in Depression." *Philosophical Transactions of the Royal Society B: Biological Sciences* 371(1708):20160011. doi: 10.1098/rstb.2016.0011.

Barrett, Lisa Feldman, and W. Kyle Simmons. 2015. "Interoceptive Predictions in the Brain." *Nature Reviews Neuroscience* 16(7):419–29. doi: 10.1038/nrn3950.

Berntson, Gary G., and Sahib S. Khalsa. 2021. "Neural Circuits of Interoception." *Trends in Neurosciences* 44(1):17–28. doi: 10.1016/j.tins.2020.09.011.

Birba, Agustina, Hernando Santamaría-García, Pavel Prado, Josefina Cruzat, Agustín Sainz Ballesteros, Agustina Legaz, Sol Fittipaldi, Claudia Duran-Aniotz, Andrea Slachevsky, Rodrigo Santibañez, Mariano Sigman, Adolfo M. García, Robert Whelan, Sebastián Moguilner, and Agustín Ibáñez. 2022. "Allostatic-Interoceptive Overload in Frontotemporal Dementia." *Biological Psychiatry* 92(1):54–67. doi: 10.1016/j.biopsych.2022.02.955.

Birn, Rasmus M., Monica A. Smith, Tyler B. Jones, and Peter A. Bandettini. 2008. "The Respiration Response Function: The Temporal Dynamics of FMRI Signal Fluctuations Related to Changes in Respiration." *NeuroImage* 40(2):644–54. doi: 10.1016/j.neuroimage.2007.11.059.

Bonaz, Bruno, Richard D. Lane, Michael L. Oshinsky, Paul J. Kenny, Rajita Sinha, Emeran A. Mayer, and Hugo D. Critchley. 2021. "Diseases, Disorders, and Comorbidities of Interoception." *Trends in Neurosciences* 44(1):39–51. doi: 10.1016/j.tins.2020.09.009.

Bowring, Alexander, Camille Maumet, and Thomas E. Nichols. 2019. "Exploring the Impact of Analysis Software on Task FMRI Results." *Human Brain Mapping* 40(11):3362–84. doi: 10.1002/hbm.24603.

Brefczynski, Julie A., and Edgar A. DeYoe. 1999. "A Physiological Correlate of the 'spotlight' of Visual Attention." *Nature Neuroscience* 2(4):370–74. doi: 10.1038/7280.

Burrows, Kaiping, Danielle C. DeVille, Kelly T. Cosgrove, Rayus T. Kuplicki, Tulsa 1000 Investigators, Martin P. Paulus, Robin Aupperle, Sahib S. Khalsa, and Jennifer L. Stewart. 2022. "Impact of Serotonergic Medication on Interoception in Major Depressive Disorder." *Biological Psychology* 169:108286. doi: 10.1016/j.biopsycho.2022.108286.

Campbell-Sills, Laura, Sonya B. Norman, Michelle G. Craske, Greer Sullivan, Ariel J. Lang, Denise A. Chavira, Alexander Bystritsky, Cathy Sherbourne, Peter Roy-Byrne, and Murray B. Stein. 2009. "Validation of a Brief Measure of Anxiety-Related Severity and Impairment: The Overall Anxiety Severity and Impairment Scale (OASIS)." *Journal of Affective Disorders* 112(1–3):92–101. doi: 10.1016/j.jad.2008.03.014.

Cannon, W. B. 1939. *The Wisdom of the Body, 2nd Ed*. Oxford, England: Norton & Co.

Carvalho, Gil B., and Antonio Damasio. 2021. "Interoception and the Origin of Feelings: A New Synthesis." *BioEssays: News and Reviews in Molecular, Cellular and Developmental Biology* 43(6):e2000261. doi: 10.1002/bies.202000261.

Cauda, Franco, Federico D'Agata, Katiuscia Sacco, Sergio Duca, Giuliano Geminiani, and Alessandro Vercelli. 2011. "Functional Connectivity of the Insula in the Resting Brain." *NeuroImage* 55(1):8–23. doi: 10.1016/j.neuroimage.2010.11.049.

Clark, Andy. 2013. "Whatever next? Predictive Brains, Situated Agents, and the Future of Cognitive Science." *The Behavioral and Brain Sciences* 36(3):181–204. doi: 10.1017/S0140525X12000477.

Clark, Andy. 2016. "Attention Alters Predictive Processing." *The Behavioral and Brain Sciences* 39:e234. doi: 10.1017/S0140525X15002472.

Corbetta, Maurizio, Gaurav Patel, and Gordon L. Shulman. 2008. "The Reorienting System of the Human Brain: From Environment to Theory of Mind." *Neuron* 58(3):306–24. doi: 10.1016/j.neuron.2008.04.017.

Cox, R. W. 1996. "AFNI: Software for Analysis and Visualization of Functional Magnetic Resonance Neuroimages." *Computers and Biomedical Research, an International Journal* 29(3):162–73. doi: 10.1006/cbmr.1996.0014.

Cox, Robert W. 2019. "Equitable Thresholding and Clustering (ETAC): A Novel Method for FMRI Clustering in AFNI." *BioRxiv* 295931. doi: 10.1101/295931.

Craig, A. D. 2002. “How Do You Feel? Interoception: The Sense of the Physiological Condition of the Body.” *Nature Reviews. Neuroscience* 3(8):655–66. doi: 10.1038/nrn894.

Craig, A. D. (Bud). 2005. “Forebrain Emotional Asymmetry: A Neuroanatomical Basis?” *Trends in Cognitive Sciences* 9(12):566–71. doi: 10.1016/j.tics.2005.10.005.

Craig, A. D. Bud. 2009. “How Do You Feel--Now? The Anterior Insula and Human Awareness.” *Nature Reviews. Neuroscience* 10(1):59–70. doi: 10.1038/nrn2555.

Critchley, Hugo D., and Sarah N. Garfinkel. 2017. “Interoception and Emotion.” *Current Opinion in Psychology* 17:7–14. doi: 10.1016/j.copsyc.2017.04.020.

Critchley, Hugo D., Christopher J. Mathias, and Raymond J. Dolan. 2002. “Fear Conditioning in Humans: The Influence of Awareness and Autonomic Arousal on Functional Neuroanatomy.” *Neuron* 33(4):653–63. doi: 10.1016/s0896-6273(02)00588-3.

Davidson, Richard J., William Irwin, Richard J. Davidson, William Irwin, Richard J. Davidson, and William Irwin. 1999. “The Functional Neuroanatomy of Emotion and Affective Style.” *Trends in Cognitive Sciences* 3(1):11–21. doi: 10.1016/S1364-6613(98)01265-0.

Davidson, Richard J., Alexander J. Shackman, and Jeffrey S. Maxwell. 2004. “Asymmetries in Face and Brain Related to Emotion.” *Trends in Cognitive Sciences* 8(9):389–91. doi: 10.1016/j.tics.2004.07.006.

De la Cruz, Feliberto, Adam R. Teed, Rachel C. Lapidus, Valerie Upshaw, Andy Schumann, Martin P. Paulus, Karl-Jürgen Bär, and Sahib S. Khalsa. 2023. “Central Autonomic Network Alterations in Anorexia Nervosa Following Peripheral Adrenergic Stimulation.” *Biological Psychiatry. Cognitive Neuroscience and Neuroimaging* 8(7):720–30. doi: 10.1016/j.bpsc.2022.12.009.

Drane, Daniel L., Negar Fani, Mark Hallett, Sahib S. Khalsa, David L. Perez, and Nicole A. Roberts. 2020. “A Framework for Understanding the Pathophysiology of Functional Neurological Disorder.” *CNS Spectrums* 1–7. doi: 10.1017/S1092852920001789.

Dum, Richard P., David J. Levinthal, and Peter L. Strick. 2009. “The Spinothalamic System Targets Motor and Sensory Areas in the Cerebral Cortex of Monkeys.” *Journal of Neuroscience* 29(45):14223–35. doi: 10.1523/JNEUROSCI.3398-09.2009.

Evrard, Henry C. 2019. “The Organization of the Primate Insular Cortex.” *Frontiers in Neuroanatomy* 13:43. doi: 10.3389/fnana.2019.00043.

Fan, Lingzhong, Hai Li, Junjie Zhuo, Yu Zhang, Jiaojian Wang, Liangfu Chen, Zhengyi Yang, Congying Chu, Sangma Xie, Angela R. Laird, Peter T. Fox, Simon B. Eickhoff, Chunshui Yu, and Tianzi Jiang. 2016. “The Human Brainnetome Atlas: A New Brain Atlas Based on Connectional Architecture.” *Cerebral Cortex* 26(8):3508–26. doi: 10.1093/cercor/bhw157.

Fermin, Alan S. R., Karl Friston, and Shigeto Yamawaki. n.d. “An Insula Hierarchical Network Architecture for Active Interoceptive Inference.” *Royal Society Open Science* 9(6):220226. doi: 10.1098/rsos.220226.

1028 Gehrlach, Daniel A., Caroline Weiand, Thomas N. Gaitanos, Eunjae Cho, Alexandra S. Klein, Alexandru A.
1029 Hennrich, Karl-Klaus Conzelmann, and Nadine Gogolla. 2020. "A Whole-Brain Connectivity Map
1030 of Mouse Insular Cortex." *ELife* 9:e55585. doi: 10.7554/eLife.55585.

1031 Ghaziri, Jimmy, Alan Tucholka, Gabriel Girard, Olivier Boucher, Jean-Christophe Houde, Maxime
1032 Descoteaux, Sami Obaid, Guillaume Gilbert, Isabelle Rouleau, and Dang Khoa Nguyen. 2018.
1033 "Subcortical Structural Connectivity of Insular Subregions." *Scientific Reports* 8(1):8596. doi:
1034 10.1038/s41598-018-26995-0.

1035 Ghaziri, Jimmy, Alan Tucholka, Gabriel Girard, Jean-Christophe Houde, Olivier Boucher, Guillaume
1036 Gilbert, Maxime Descoteaux, Sarah Lippé, Pierre Rainville, and Dang Khoa Nguyen. 2017. "The
1037 Corticocortical Structural Connectivity of the Human Insula." *Cerebral Cortex* 27(2):1216–28. doi:
1038 10.1093/cercor/bhv308.

1039 Glover, Gary H., Tie-Qiang Li, and David Ress. 2000. "Image-Based Method for Retrospective Correction
1040 of Physiological Motion Effects in FMRI: RETROICOR." *Magnetic Resonance in Medicine*
1041 44(1):162–67. doi: 10.1002/1522-2594(200007)44:1<162::AID-MRM23>3.0.CO;2-E.

1042 Gogolla, Nadine. 2017. "The Insular Cortex." *Current Biology: CB* 27(12):R580–86. doi:
1043 10.1016/j.cub.2017.05.010.

1044 Goldstein-Piekarski, Andrea N., Tali M. Ball, Zoe Samara, Brooke R. Staveland, Arielle S. Keller, Scott L.
1045 Fleming, Katherine A. Grisanzio, Bailey Holt-Gosselin, Patrick Stetz, Jun Ma, and Leanne M.
1046 Williams. 2022. "Mapping Neural Circuit Biotypes to Symptoms and Behavioral Dimensions of
1047 Depression and Anxiety." *Biological Psychiatry* 91(6):561–71. doi:
1048 10.1016/j.biopsych.2021.06.024.

1049 Halani, Priyanka Kadam, Uduak U. Andy, Hengyi Rao, and Lily A. Arya. 2020. "Regions of the Brain
1050 Activated in Bladder Filling vs Rectal Distention in Healthy Adults: A Meta-Analysis of
1051 Neuroimaging Studies." *Neurourology and Urodynamics* 39(1):58–65. doi: 10.1002/nau.24221.

1052 Harrison, Olivia K., Laura Köchli, Stephanie Marino, Roger Luechinger, Franciszek Hennel, Katja Brand,
1053 Alexander J. Hess, Stefan Frässle, Sandra Iglesias, Fabien Vinckier, Frederike H. Petzschner,
1054 Samuel J. Harrison, and Klaas E. Stephan. 2021. "Interoception of Breathing and Its Relationship
1055 with Anxiety." *Neuron* 109(24):4080-4093.e8. doi: 10.1016/j.neuron.2021.09.045.

1056 Hassanpour, Mahlega S., W. Kyle Simmons, Justin S. Feinstein, Qingfei Luo, Rachel C. Lapidus, Jerzy
1057 Bodurka, Martin P. Paulus, and Sahib S. Khalsa. 2018. "The Insular Cortex Dynamically Maps
1058 Changes in Cardiorespiratory Interoception." *Neuropsychopharmacology* 43(2):426–34. doi:
1059 10.1038/npp.2017.154.

1060 Hassanpour, Mahlega S., Lirong Yan, Danny J. J. Wang, Rachel C. Lapidus, Armen C. Arevian, W. Kyle
1061 Simmons, Jamie D. Feusner, and Sahib S. Khalsa. 2016. "How the Heart Speaks to the Brain:
1062 Neural Activity during Cardiorespiratory Interoceptive Stimulation." *Philosophical Transactions*
1063 *of the Royal Society B: Biological Sciences* 371(1708):20160017. doi: 10.1098/rstb.2016.0017.

1064 Hatton, Sean N., Jim Lagopoulos, Daniel F. Hermens, Sharon L. Naismith, Maxwell R. Bennett, and Ian B.
1065 Hickie. 2012. "Correlating Anterior Insula Gray Matter Volume Changes in Young People with

Clinical and Neurocognitive Outcomes: An MRI Study." *BMC Psychiatry* 12(1):45. doi: 10.1186/1471-244X-12-45.

Henseler, Ilona, Sebastian Krüger, Peter Dechent, and Oliver Gruber. 2011. "A Gateway System in Rostral PFC? Evidence from Biasing Attention to Perceptual Information and Internal Representations." *NeuroImage* 56(3):1666–76. doi: 10.1016/j.neuroimage.2011.02.056.

Hommel, Bernhard, Craig S. Chapman, Paul Cisek, Heather F. Neyedli, Joo-Hyun Song, and Timothy N. Welsh. 2019. "No One Knows What Attention Is." *Attention, Perception, & Psychophysics* 81(7):2288–2303. doi: 10.3758/s13414-019-01846-w.

Jänig, Wilfrid. 2006. *Integrative Action of the Autonomic Nervous System: Neurobiology of Homeostasis*. Cambridge: Cambridge University Press.

Jänig, Wilfrid, Janet R. Keast, Elspeth M. McLachlan, Winfried L. Neuhuber, and Michelle Southard-Smith. 2017. "Renaming All Spinal Autonomic Outflows as Sympathetic Is a Mistake." *Autonomic Neuroscience: Basic & Clinical* 206:60–62. doi: 10.1016/j.autneu.2017.04.003.

Jo, Hang Joon, Ziad S. Saad, W. Kyle Simmons, Lydia A. Milbury, and Robert W. Cox. 2010. "Mapping Sources of Correlation in Resting State FMRI, with Artifact Detection and Removal." *NeuroImage* 52(2):571–82. doi: 10.1016/j.neuroimage.2010.04.246.

Kasper, Lars, Maria Engel, Jakob Heinzle, Matthias Mueller-Schrader, Nadine N. Graedel, Jonas Reber, Thomas Schmid, Christoph Barmet, Bertram J. Wilm, Klaas Enno Stephan, and Klaas P. Pruessmann. 2022. "Advances in Spiral FMRI: A High-Resolution Study with Single-Shot Acquisition." *NeuroImage* 246:118738. doi: 10.1016/j.neuroimage.2021.118738.

Kerr, Kara L., Scott E. Moseman, Jason A. Avery, Jerzy Bodurka, Nancy L. Zucker, and W. Kyle Simmons. 2016. "Altered Insula Activity during Visceral Interoception in Weight-Restored Patients with Anorexia Nervosa." *Neuropsychopharmacology* 41(2):521–28. doi: 10.1038/npp.2015.174.

Khalsa, Sahib S., Ralph Adolphs, Oliver G. Cameron, Hugo D. Critchley, Paul W. Davenport, Justin S. Feinstein, Jamie D. Feusner, Sarah N. Garfinkel, Richard D. Lane, Wolf E. Mehling, Alicia E. Meuret, Charles B. Nemeroff, Stephen Oppenheimer, Frederike H. Petzschner, Olga Pollatos, Jamie L. Rhudy, Lawrence P. Schramm, W. Kyle Simmons, Murray B. Stein, Klaas E. Stephan, Omer Van den Bergh, Ilse Van Diest, Andreas von Leupoldt, Martin P. Paulus, Vivien Ainley, Obada Al Zoubi, Robin Aupperle, Jason Avery, Leslie Baxter, Christoph Benke, Laura Berner, Jerzy Bodurka, Eric Breese, Tiffany Brown, Kaiping Burrows, Yoon-Hee Cha, Ashley Clausen, Kelly Cosgrove, Danielle Deville, Laramie Duncan, Patrice Duquette, Hamed Ekhtiari, Thomas Fine, Bart Ford, Indira Garcia Cordero, Diamond Gleghorn, Yvette Guereca, Neil A. Harrison, Mahlega Hassanpour, Tanja Hechler, Aaron Heller, Natalie Hellman, Beate Herbert, Behnaz Jarrahi, Kara Kerr, Namik Kirlic, Megan Klabunde, Thomas Kraynak, Michael Kriegsman, Juliet Kroll, Rayus Kuplicki, Rachel Lapidus, Trang Le, Kyle Logie Hagen, Ahmad Mayeli, Amanda Morris, Nasir Naqvi, Kristina Oldroyd, Christiane Pané-Farré, Raquel Phillips, Tasha Poppa, Willliam Potter, Maria Puhl, Adam Safron, Margaret Sala, Jonathan Savitz, Heather Saxon, Will Schoenhals, Colin Stanwell-Smith, Adam Teed, Yuri Terasawa, Katie Thompson, Marisa Toups, Satoshi Umeda, Valerie Upshaw, Teresa Victor, Christina Wierenga, Colleen Wohlrab, Hung-wen Yeh, Adrian Yoris, Fadel Zeidan, Vadim Zotev, and Nancy Zucker. 2018. "Interoception and Mental Health: A

Roadmap." *Biological Psychiatry: Cognitive Neuroscience and Neuroimaging* 3(6):501–13. doi: 10.1016/j.bpsc.2017.12.004.

Khalsa, Sahib S., and Rachel C. Lapidus. 2016. "Can Interoception Improve the Pragmatic Search for Biomarkers in Psychiatry?" *Frontiers in Psychiatry* 7. doi: 10.3389/fpsyt.2016.00121.

Khalsa, Sahib S., David Rudrauf, Justin S. Feinstein, and Daniel Tranel. 2009. "The Pathways of Interoceptive Awareness." *Nature Neuroscience* 12(12):1494–96. doi: 10.1038/nn.2411.

Kimmerly, Derek S., Deborah D. O'Leary, Ravi S. Menon, Joseph S. Gati, Kevin Shoemaker. 2005. "Cortical regions associated with autonomic cardiovascular regulation during lower body negative pressure in humans." *Journal of Physiology* 569(1):331-345. https://doi.org/10.1113/jphysiol.2005.091637

Knudsen, Lasse, Christopher J. Bailey, Jakob U. Blicher, Yan Yang, Peng Zhang, and Torben E. Lund. 2023. "Improved Sensitivity and Microvascular Weighting of 3T Laminar FMRI with GE-BOLD Using NORDIC and Phase Regression." *NeuroImage* 271:120011. doi: 10.1016/j.neuroimage.2023.120011.

Kroenke, K., R. L. Spitzer, and J. B. Williams. 2001. "The PHQ-9: Validity of a Brief Depression Severity Measure." *Journal of General Internal Medicine* 16(9):606–13. doi: 10.1046/j.1525-1497.2001.016009606.x.

Kutz, Amanda M., Alison G. Marsh, Craig G. Gunderson, Shira Maguen, and Robin M. Masheb. 2020. "Eating Disorder Screening: A Systematic Review and Meta-Analysis of Diagnostic Test Characteristics of the SCOFF." *Journal of General Internal Medicine* 35(3):885–93. doi: 10.1007/s11606-019-05478-6.

Mayeli, Ahmad, Obada Al Zoubi, Evan J. White, Sheridan Chappelle, Rayus Kuplicki, Alexa Morton, Jaimee Bruce, Ryan Smith, Justin S. Feinstein, Jerzy Bodurka, Martin P. Paulus, and Sahib S. Khalsa. 2023. "Parieto-Occipital ERP Indicators of Gut Mechanosensation in Humans." *Nature Communications* 14(1):3398. doi: 10.1038/s41467-023-39058-4.

Mechelli, Andrea, Cathy J. Price, Karl J. Friston, and Alumit Ishai. 2004. "Where Bottom-up Meets Top-down: Neuronal Interactions during Perception and Imagery." *Cerebral Cortex (New York, N.Y.: 1991)* 14(11):1256–65. doi: 10.1093/cercor/bhh087.

Mufson, Elliott J., and M.-Marsel Mesulam. 1982. "Insula of the Old World Monkey. II: Afferent Cortical Input and Comments on the Claustrum." *Journal of Comparative Neurology* 212(1):23–37. doi: https://doi.org/10.1002/cne.902120103.

Murphy, Fionnuala C., Ian Nimmo-Smith, and Andrew D. Lawrence. 2003. "Functional Neuroanatomy of Emotions: A Meta-Analysis." *Cognitive, Affective, & Behavioral Neuroscience* 3(3):207–33. doi: 10.3758/CABN.3.3.207.

Nord, Camilla L., Rebecca P. Lawson, and Tim Dalgleish. 2021. "Disrupted Dorsal Mid-Insula Activation During Interoception Across Psychiatric Disorders." *The American Journal of Psychiatry* 178(8):761–70. doi: 10.1176/appi.ajp.2020.20091340.

Oppenheimer, S. M., A. Gelb, J. P. Girvin, and V. C. Hachinski. 1992. “Cardiovascular Effects of Human Insular Cortex Stimulation.” *Neurology* 42(9):1727–32. doi: 10.1212/wnl.42.9.1727.

Oppenheimer, Stephen M., Adrian Gelb, John P. Girvin, and Vladimir C. Hachinski. 1992. “Cardiovascular Effects of Human Insular Cortex Stimulation.” *Neurology* 42(9):1727–1727. doi: 10.1212/WNL.42.9.1727.

Pace-Schott, Edward F., Marlissa C. Amole, Tatjana Aue, Michela Balconi, Lauren M. Bylsma, Hugo Critchley, Heath A. Demaree, Bruce H. Friedman, Anne Elizabeth Kotynski Gooding, Olivia Gosseries, Tanja Jovanovic, Lauren A. J. Kirby, Kasia Kozlowska, Steven Laureys, Leroy Lowe, Kelsey Magee, Marie-France Marin, Amanda R. Merner, Jennifer L. Robinson, Robert C. Smith, Derek P. Spangler, Mark Van Overveld, and Michael B. VanElzakker. 2019. “Physiological Feelings.” *Neuroscience and Biobehavioral Reviews* 103:267–304. doi: 10.1016/j.neubiorev.2019.05.002.

Paulus, Martin P., Justin S. Feinstein, and Sahib S. Khalsa. 2019. “An Active Inference Approach to Interoceptive Psychopathology.” *Annual Review of Clinical Psychology* 15:97–122. doi: 10.1146/annurev-clinpsy-050718-095617.

Paulus, Martin P., and Sahib S. Khalsa. 2021. “When You Don’t Feel Right Inside: Homeostatic Dysregulation and the Mid-Insular Cortex in Psychiatric Disorders.” *The American Journal of Psychiatry* 178(8):683–85. doi: 10.1176/appi.ajp.2021.21060622.

Petzschner, Frederike H., Sarah N. Garfinkel, Martin P. Paulus, Christof Koch, and Sahib S. Khalsa. 2021. “Computational Models of Interoception and Body Regulation.” *Trends in Neurosciences* 44(1):63–76. doi: 10.1016/j.tins.2020.09.012.

Pezzulo, Giovanni, Laura Barca, and Karl J. Friston. 2015. “Active Inference and Cognitive-Emotional Interactions in the Brain.” *Behavioral and Brain Sciences* 38:e85. doi: 10.1017/S0140525X14001009.

Picard, Rosalind W., Szymon Fedor, and Yadid Ayzenberg. 2016. “Multiple Arousal Theory and Daily-Life Electrodermal Activity Asymmetry.” *Emotion Review* 8(1):62–75. doi: 10.1177/1754073914565517.

Pohl, R., V. K. Yeragani, R. Balon, J. M. Rainey, H. Lycaki, A. Ortiz, R. Berchou, and P. Weinberg. 1988. “Isoproterenol-Induced Panic Attacks.” *Biological Psychiatry* 24(8):891–902. doi: 10.1016/0006-3223(88)90224-7.

Pollatos, Olga, Rainer Schandry, Dorothee P. Auer, and Christian Kaufmann. 2007. “Brain Structures Mediating Cardiovascular Arousal and Interoceptive Awareness.” *Brain Research* 1141:178–87. doi: 10.1016/j.brainres.2007.01.026.

Rauss, Karsten, and Gilles Pourtois. 2013. “What Is Bottom-Up and What Is Top-Down in Predictive Coding?” *Frontiers in Psychology* 4:276. doi: 10.3389/fpsyg.2013.00276.

Schulz, Stefan M. 2016. “Neural Correlates of Heart-Focused Interoception: A Functional Magnetic Resonance Imaging Meta-Analysis.” *Philosophical Transactions of the Royal Society B: Biological Sciences* 371(1708):20160018. doi: 10.1098/rstb.2016.0018.

Seth, Anil K., and Karl J. Friston. 2016. “Active Interoceptive Inference and the Emotional Brain.” *Philosophical Transactions of the Royal Society of London. Series B, Biological Sciences* 371(1708):20160007. doi: 10.1098/rstb.2016.0007.

Sheehan, D. V., Y. Lecrubier, K. H. Sheehan, P. Amorim, J. Janavs, E. Weiller, T. Hergueta, R. Baker, and G. C. Dunbar. 1998. “The Mini-International Neuropsychiatric Interview (M.I.N.I.): The Development and Validation of a Structured Diagnostic Psychiatric Interview for DSM-IV and ICD-10.” *The Journal of Clinical Psychiatry* 59 Suppl 20:22-33;quiz 34-57.

Shipley, Michael T., and Marc S. Sanders. 1982. “Special Senses Are Really Special: Evidence for a Reciprocal, Bilateral Pathway between Insular Cortex and Nucleus Parabrachialis.” *Brain Research Bulletin* 8(5):493–501. doi: 10.1016/0361-9230(82)90007-7.

Simmons, W. Kyle, Jason A. Avery, Joel C. Barcalow, Jerzy Bodurka, Wayne C. Drevets, and Patrick Bellgowan. 2013. “Keeping the Body in Mind: Insula Functional Organization and Functional Connectivity Integrate Interoceptive, Exteroceptive, and Emotional Awareness.” *Human Brain Mapping* 34(11):2944–58. doi: 10.1002/hbm.22113.

Smith, Ryan, Rayus Kuplicki, Justin Feinstein, Katherine L. Forthman, Jennifer L. Stewart, Martin P. Paulus, Tulsa 1000 Investigators, and Sahib S. Khalsa. 2020. “A Bayesian Computational Model Reveals a Failure to Adapt Interoceptive Precision Estimates across Depression, Anxiety, Eating, and Substance Use Disorders.” *PLOS Computational Biology* 16(12):e1008484. doi: 10.1371/journal.pcbi.1008484.

Smith, Ryan, Julian F. Thayer, Sahib S. Khalsa, and Richard D. Lane. 2017. “The Hierarchical Basis of Neurovisceral Integration.” *Neuroscience & Biobehavioral Reviews* 75:274–96. doi: 10.1016/j.neubiorev.2017.02.003.

Song, Xiaopeng, Bhaswati Roy, Gregg C. Fonarow, Mary A. Woo, Rajesh Kumar. 2018. "Brain structural changes associated with aberrant functional responses to the Valsalva maneuver in heart failure. *Journal of Neuroscience Research* 96(9). https://doi.org/10.1002/jnr.24264

Spitzer, Robert L., Kurt Kroenke, Janet B. W. Williams, and Bernd Löwe. 2006. “A Brief Measure for Assessing Generalized Anxiety Disorder: The GAD-7.” *Archives of Internal Medicine* 166(10):1092–97. doi: 10.1001/archinte.166.10.1092.

Sterling, Peter. 2012. “Allostasis: A Model of Predictive Regulation.” *Physiology & Behavior* 106(1):5–15. doi: 10.1016/j.physbeh.2011.06.004.

Stewart, Jennifer L., Sahib S. Khalsa, Rayus Kuplicki, Maria Puhl, T1000 Investigators, and Martin P. Paulus. 2020. “Interoceptive Attention in Opioid and Stimulant Use Disorder.” *Addiction Biology* 25(6):e12831. doi: https://doi.org/10.1111/adb.12831.

Sylvester, Ching-Yune C., Tor D. Wager, Steven C. Lacey, Luis Hernandez, Thomas E. Nichols, Edward E. Smith, and John Jonides. 2003. “Switching Attention and Resolving Interference: FMRI Measures of Executive Functions.” *Neuropsychologia* 41(3):357–70. doi: 10.1016/s0028-3932(02)00167-7.

Teed, Adam R., Justin S. Feinstein, Maria Puhl, Rachel C. Lapidus, Valerie Upshaw, Rayus T. Kuplicki, Jerzy Bodurka, Olujimi A. Ajijola, Walter H. Kaye, Wesley K. Thompson, Martin P. Paulus, and Sahib S.

1219 Khalsa. 2022. “Association of Generalized Anxiety Disorder With Autonomic Hypersensitivity and
1220 Blunted Ventromedial Prefrontal Cortex Activity During Peripheral Adrenergic Stimulation: A
1221 Randomized Clinical Trial.” *JAMA Psychiatry* 79(4):323–32. doi:
1222 10.1001/jamapsychiatry.2021.4225.

1223 Uddin, Lucina Q., Joshua Kinnison, Luiz Pessoa, and Michael L. Anderson. 2014. “Beyond the Tripartite
1224 Cognition–Emotion–Interoception Model of the Human Insular Cortex.” *Journal of Cognitive*
1225 *Neuroscience* 26(1):16–27. doi: 10.1162/jocn_a_00462.

1226 White, Lauren K., Jennifer C. Britton, Stefanie Sequeira, Emily G. Ronkin, Gang Chen, Yair Bar-Haim,
1227 Tomer Shechner, Monique Ernst, Nathan A. Fox, Ellen Leibenluft, and Daniel S. Pine. 2016.
1228 “Behavioral and Neural Stability of Attention Bias to Threat in Healthy Adolescents.”
1229 *NeuroImage* 136:84–93. doi: 10.1016/j.neuroimage.2016.04.058.

1230 Wiestler, Tobias, and Jörn Diedrichsen. 2013. “Skill Learning Strengthens Cortical Representations of
1231 Motor Sequences” edited by J. C. Culham. *ELife* 2:e00801. doi: 10.7554/eLife.00801.

1232 Wu, Yu, Changwan Chen, Ming Chen, Kai Qian, Xinyou Lv, Haiting Wang, Lifei Jiang, Lina Yu, Min Zhuo,
1233 and Shuang Qiu. 2020. “The Anterior Insular Cortex Unilaterally Controls Feeding in Response to
1234 Aversive Visceral Stimuli in Mice.” *Nature Communications* 11(1):640. doi: 10.1038/s41467-020-
1235 14281-5.

1236